



HAL
open science

Injectable bone cement containing carboxymethyl cellulose microparticles as a silver delivery system able to reduce implant-associated infection risk

Sylvaine Jacquart, Sophie Girod-Fullana, Fabien Brouillet, Christel Pigasse, Robin Siadous, Mohamed Fatnassi, Julien Grimoud, Christian Rey, Christine Roques, Christèle Combes

► To cite this version:

Sylvaine Jacquart, Sophie Girod-Fullana, Fabien Brouillet, Christel Pigasse, Robin Siadous, et al.. Injectable bone cement containing carboxymethyl cellulose microparticles as a silver delivery system able to reduce implant-associated infection risk. *Acta Biomaterialia*, 2022, 145, pp.342-357. 10.1016/J.ACTBIO.2022.04.015 . hal-03930203

HAL Id: hal-03930203

<https://cnrs.hal.science/hal-03930203>

Submitted on 2 Jun 2023

HAL is a multi-disciplinary open access archive for the deposit and dissemination of scientific research documents, whether they are published or not. The documents may come from teaching and research institutions in France or abroad, or from public or private research centers.

L'archive ouverte pluridisciplinaire **HAL**, est destinée au dépôt et à la diffusion de documents scientifiques de niveau recherche, publiés ou non, émanant des établissements d'enseignement et de recherche français ou étrangers, des laboratoires publics ou privés.

Injectable bone cement containing carboxymethyl cellulose microparticles as a silver delivery system able to reduce implant- associated infection risk

Sylvaine Jacquart^a, Sophie Girod-Fullana^b, Fabien Brouillet^b, Christel Pigasse^c, Robin Siadous^d, Mohamed Fatnassi^a, Julien Grimoud^c, Christian Rey^a, Christine Roques^{c,e}, Christèle Combes^{a,*}

^aCIRIMAT, Université de Toulouse, CNRS, Toulouse INP - ENSIACET, Toulouse, France

^bCIRIMAT, Université de Toulouse, CNRS, Université Toulouse 3 - Paul Sabatier, Toulouse, France

^cLaboratoire de Génie Chimique, Université de Toulouse, CNRS, INPT, Université Toulouse 3 - Paul Sabatier, Toulouse, France

^dUniversité de Bordeaux, Inserm U1026 Bioingénierie Tissulaire (BioTis), Bordeaux, France

^eCHU Toulouse, Hôpital Purpan, Service de Bactériologie-Hygiène, Toulouse, France

*Corresponding author: Christèle COMBES
ENSIACET - CIRIMAT
4 allée Emile Monso
31030 Toulouse cedex 4
France
E-mail address: christele.combes@ensiacet.fr
Tel : +33 (0)5 34 32 34 09

Abstract

In the challenging quest for a solution to reduce the risk of implant-associated infections in bone substitution surgery, the use of silver ions is promising regarding its broad spectrum on planktonic, sessile as well as multiresistant bacteria. In view of controlling its delivery *in situ* at the desired dose, we investigated its encapsulation in carboxymethyl cellulose (CMC) microparticles by spray-drying and included the latter in the formulation of a self-setting calcium phosphate bone cement. We implemented an original step-by-step methodology starting from the *in vitro* study of the antibacterial properties and cytotoxicity of two silver salts of different solubility in aqueous medium and then in the cement to determine the range of silver loading able to confer anti-biofilm and non-cytotoxic properties to the biomaterial. A dose-dependent efficiency of silver was demonstrated on the main species involved in bone-implant infection (*S. aureus* and *S. epidermidis*). Loading silver in microspheres instead of loading it directly inside the cement permitted to avoid undesired silver-cement interactions during setting and led to a faster release of silver, *i.e.* to a higher dose released within the first days combining anti-biofilm activity and preserved cytocompatibility. In addition, a combined interest of the introduction of about 10% (w/w) silver-loaded CMC microspheres in the cement formulation was demonstrated leading to a fully injectable and highly porous (77%) cement, showing a compressive strength analogous to cancellous bone. This injectable silver-loaded biomimetic composite cement formulation constitutes a versatile bone substitute material with tunable drug delivery properties, able to fight against bone implant associated infection.

Keywords: silver salts, encapsulation, controlled release, bone cements, anti-biofilm activity, injectability.

1. Introduction

The burden of implant-associated infections (IAIs) in surgery has grown together with the number of implanted medical devices [1-2]. IAIs emergence involved bacterial adhesion and then formation of a protective biofilm by microorganisms mainly introduced intra-operatively but also post-operatively. Regarding orthopedic surgeries, the common microorganisms associated with implant infections are Gram-positive bacteria such as *Staphylococcus aureus*, *Staphylococcus epidermidis* (50 to 60%) then *Enterococcus faecalis* and to a less extent Gram-negative bacteria, e.g., *Pseudomonas aeruginosa*, including bacteria with acquired resistance [3]. Current clinical treatments of microbial infections rely on systemic antibiotics, but the increasing tolerance to antibiotics [4-6] and biofilm formation with reduced susceptibility to host defenses and antimicrobial therapies thus challenge IAIs management and leading failure in their treatment [7-9]. Control of infection on and around implants is usually difficult and preventive measures are sought by the researchers to overcome implant-related colonization then infection. Various approaches have been attempted to make implant surface anti-adherent / antibacterial or to embedded antibacterial compounds inside the implant [10-12].

Among antimicrobials tested for coating implants silver is considered promising regarding its broad spectrum including planktonic and sessile Gram positive and Gram negative bacteria, as well as multiresistant bacteria, including methicillin-resistant staphylococci [13-18]. Combination of various mechanisms of action including impact on the respiratory chain [19-21] underlines the interest of using silver-doped bone substitute materials to prevent IAIs. Different studies support this hypothesis based on controlled release of Ag⁺, biodegradation and antimicrobial activity [22-23].

In orthopaedics, silver-coated devices showed a trend toward reduction of infections [24-26]. In 2016, Kuehl *et al.* [27] demonstrated that silver-coated TiAlNb alloy cages, alone or associated to daptomycin or vancomycin, effectively prevented IAIs by *S. epidermidis in vivo*. Authors also observed no emergence of silver resistance in several strains of staphylococci after 50 passages, thus concluded that silver coating is a promising strategy for lowering the risk of IAIs.

Calcium phosphate cements (CPC) are well-known bone substitute materials that can be used as drug delivery systems favoring local release on the implantation site [28-29] and different strategies have been investigated to incorporate silver into CPC, especially as silver salts [30], Ag doped mineral phases [31-34] or through the introduction of silver nanoparticles [35]. In

particular, Jacquart *et al.* showed that calcium carbonate-calcium phosphate cement loaded with a silver salt either introduced in the liquid or the solid phase of the cement led to an antibacterial and non-cytotoxic bone cement [30]. However a very high and non-optimized concentration of silver (Ca/Ag = 10.3) was involved in the cement formulation. Moreover, this formulation was not injectable whereas injectable formulations favors implementation of mini-invasive surgery techniques which may be a decisive advantage to fight against IAIs compare to conventional bone cements implantation.

Loaded natural- or synthetic polymer-based microparticles [36-39] incorporation into the CPC is of interest as it can combine drug release and cement properties optimization such as paste injectability, cohesion, and resorption once implanted [28, 40-48].

Synthetic polymers, especially poly(lactic-*co*-glycolic) acid (PLGA), have been extensively used for this purpose [38, 40-41, 44, 47, 49]. However, the acidic degradation of polyesters remains problematic [47]. Other polymers can advantageously play the role of drug reservoir [50], such as gelatin [39, 48, 51] and more rarely polysaccharides [36, 43, 52]. The complementary contribution of the latter as rheological modifiers or cohesion promoters is advantageous in cement formulation [45-46, 52-55], and our team has demonstrated their interest in terms of drug release control [36, 43]. Among polysaccharides, cellulosic derivatives are well-known release modifiers in pharmaceutical formulation, with a GRAS status [56]. In particular, carboxymethyl cellulose (CMC) has gelling properties and is adapted for microspheres elaboration [57]. However, it has never been tested in cement formulation to improve its drug loading and release properties.

In this context, we decided to evaluate CMC as a candidate to formulate a microspheres-loaded biomimetic bone cement whose Ag⁺ dose and release properties could be adapted to reduce the risk of infections at the implanted site. To reach this aim, the microspheres must combine: 1) A high silver encapsulation efficiency; 2) Controlled release properties especially regarding “race to the surface” of efficient Ag⁺ quantities for the early control of adhesion and biofilm formation by the main pathogens involved in those IAIs and introduced during the surgery (*S. aureus* and *S. epidermidis*); 3) Size distribution permitting to maintain or, even better improve cements’ main properties, and more particularly its injectability and setting ability. As a consequence, the choice of the silver dose, as well as the choice of the encapsulation process and the operating encapsulation conditions are critical points in the elaboration of such composite cement with antibacterial properties.

2. Materials and methods

2.1. Materials

Carboxymethyl cellulose CMC was kindly provided by Ashland Aqualon 7H4XF-PH (France). Commercial silver nitrate salt (AgNO_3 99.9%; Alfa Aesar[®]) and Tris (Tris(hydroxymethyl)aminomethane Trizma[®] base BioXtra (Sigma, purity \geq 99.9%) were used without further purification. Brushite (DCPD, $\text{CaHPO}_4 \cdot 2\text{H}_2\text{O}$) and vaterite (CaCO_3) and silver phosphate (Ag_3PO_4) powders used for mineral cement formulations were synthesized as previously published [30]. All other chemicals were analytical grade from Fisher Scientific.

2.2. *In vitro* methods for the evaluation of the cytotoxicity of a solution of the silver salts

The different methods associated to the *in vitro* cytotoxicity test were performed according to the ISO 10993-12 standard.

2.2.1. Human bone marrow stromal cells (hBMSCs) culture

Human bone marrow mesenchymal stem cells (hBMSCs) were isolated from human bone marrow samples (agreement with the Orthopaedic Department of Bordeaux Hospital (France) for surgical wastes collection for research use only, approved by the Bioethics Committee), as previously described [58]. Briefly, bone marrow was aspirated from the femoral diaphysis or iliac bone after obtaining consent from patients undergoing hip prosthesis surgery after trauma. Cells were separated into a single suspension by sequential passages through syringes fitted with 16-, 18- or 21-gauge needles. After centrifugation for 10 min at 800g, the pellet was resuspended in minimal essential medium (Alpha-MEM; Invitrogen) supplemented with 10% (v/v) fetal calf serum (FCS; Gibco) before cell seeding in standard cell culture plates. Once 80% confluence was reached, the cells were subcultured for cytotoxicity study. All cell cultures were performed at 37 °C in a humidified atmosphere of 5% CO_2 .

2.2.2. Samples preparation

Solutions of Ag_3PO_4 or AgNO_3 salt were prepared with 5 mg of silver salt in 1 mL of alpha MEM without FCS and then diluted at 1:10, 1:100 and 1:1000 (v/v) ratios with the same medium. Due to the lower solubility of Ag_3PO_4 salt in water (6.4 $\text{mg}\cdot\text{L}^{-1}$ at 20°C) compared with that of AgNO_3 (2160 $\text{g}\cdot\text{L}^{-1}$ at 20°C), AgNO_3 was fully dissolved in this aqueous medium

whereas some Ag_3PO_4 particles remained in suspension except for the 1:1000 v/v diluted sample.

The effect of these different conditions with six replicates for each solution on the viability and the metabolism activity of the hBMSCs was evaluated using neutral red assay and MTT assay respectively [59-60].

In order to perform the cytotoxicity assays, cells were seeded in 96-well plates at a density 2×10^4 cells per well and incubated overnight at 37°C before experiment up to semi-confluency (80% confluence). Then when culture cells were semi-confluent, they were exposed for 24 hours to a prepared medium with the different silver salt solutions and the culture medium without additional treatment was used as the control. Cell cultures were maintained under standard methodology.

2.2.3. *Neutral red assay*

After overnight incubation, plates were washed with PBS and 100 μL of medium supplemented with 10% (v/v) FCS with neutral red (5 mg/mL in distilled water) was added into each well. The cells were incubated with neutral red for 3 h at 37°C and the dye was extracted with 200 μL of a mixture of 1% acetic acid: 50% ethanol, and the absorbance was measured using a spectrophotometer at $\lambda = 550\text{ nm}$ with plate reader (PerkinElmer). The results were calculated as a percentage in relation to the untreated cells in control wells.

2.2.4. *MTT assay*

The MTT assay was employed to assess hBMSCs cell activity after treatment with the different Ag-containing solutions. Cells were seeded in 96-well plates at a density 2×10^4 cells per well and incubated overnight at 37°C before experiment. Subsequently, Ag-containing solutions were added to each well except the well with control solution and incubated for 24 h. After incubation the cells were rinsed with PBS, then 125 μL of reaction solution containing methyl thiazolyl diphenyl tetrazolium bromide solution (0.5 mg/mL) in culture medium without phenol red was added to each well. The plates were incubated for 3 h at 37°C , and then the formazan crystals were extracted with 200 μL DMSO and the absorbance was measured at 550 nm with plate reader (PerkinElmer). Cell activity was calculated as a percentage of that of the untreated cells.

The intensity of the colors obtained (red and blue respectively) is directly proportional to the viability and metabolic activity of the cell population and inversely proportional to the

toxicity of the sample. The results were expressed as a percentage of the negative control (plastic without treatment) tested during the same experiment.

The Gaussian distribution of the data has been checked by Kolmogorov-Smirnov test.

2.3. *In vitro* evaluation of the antibacterial activity of aqueous solution of silver salts and of cement pellets

The antibacterial properties of AgNO₃ and Ag₃PO₄ salts and reference and composite cements have been evaluated.

2.3.1. *Bacterial strains*

S. aureus CIP 4.83, *S. epidermidis* CIP 6821T, *S. aureus* CRBIP 21.18 (MRSA and multiresistant) (Institut Pasteur Collection, Paris, France) and *S. aureus* ATCC 33591 (MRSA) (American Type Culture Collection) were tested for MICs and MBCs determination. The two first strains were selected for assays on biofilm formation. Strains were preserved at -80°C according to the EN 12353 (2017) and subcultured on tryptic soy (Biomérieux, Craponne, France) under aerobic conditions at 36°C. Only subcultures 2 and 3 on tryptic soy agar (Biomérieux, Craponne, France) were used for assays. Before each assay, suspensions were prepared in distilled sterile water at a concentration of 5x10⁷ CFU/mL.

2.3.2. *Determination of MIC (minimal inhibitory concentration) and MBC (minimal bactericidal concentration)*

According to CASFM and EUCAST as previously described [61-62] each silver salt solution under assay was diluted using two-fold steps in microtiter plates in Muller Hinton (MH) broth (Biomérieux, Craponne, France) from column 1 to column 10. Concentration ranges expressed in ppm of silver were 4.95 - 0.01 for Ag₃PO₄ regarding its low solubility in water and 404 - 0.79 ppm for AgNO₃. Columns 11 and 12 were for sterility control (without product and without microorganism) and growth control (without product and with microorganisms), respectively. Inoculation was performed using a multipoint inoculator (Denley) under a volume of about 1.5 µL of each suspension. Then microplates were incubated at 36°C for 24 hours.

After incubation, minimal inhibitory concentration (MIC) was defined as the concentration of silver ions at which no macroscopic sign of cellular growth was detected in comparison to the control (without silver salt). Minimal bactericidal concentration (MBC) was determined after

transfer from each well to MH agar (multipoint inoculator) then incubation in conditions previously described. MBC was defined as the concentration of silver ions at which no macroscopic sign of cellular growth was detected in comparison to the control (without silver salt).

All experiments were carried out in duplicate.

2.3.3. Evaluation on biofilm formation

Preliminary experiment:

In an attempt to define the interest of silver incorporation in the composite cement and the range of concentration to be considered, the antibacterial activity was firstly investigated considering the ability of *S. aureus* CIP 4.83 to adhere and colonize microplate surfaces when Ag_3PO_4 was added at $t = 0$ with inoculation or 2 h after inoculation (to promote the adhesion step without silver). *S. aureus* CIP 4.83 was grown in 24-well microplates with/without silver (the silver concentration ranged from 0.0025 to 2.5 ppm of Ag, under the limit of solubility of Ag_3PO_4 salt) and 2 cm³ of biofilm broth (BB) as previously described by Campanac *et al.* [63] (composition: $\text{MgSO}_4 \cdot 2\text{H}_2\text{O}$ (0.2 g/L), $\text{FeSO}_4 \cdot 7\text{H}_2\text{O}$ (0.0005 g/L), Na_2HPO_4 (1.25 g/L), KH_2PO_4 (0.5 g/L), $(\text{NH}_4)_2\text{SO}_4$ (0.1 g/L), glucose (0.05 g/L), Sigma Aldrich). The model has been chosen considering that the composition of BB and the renewal of the medium promote adherent but not planktonic cells growth with a biofilm structure. After initial inoculation with 10² CFU (low inoculum chosen to mimic limited contamination risk during surgery), the adhesion step was considered at 2 h for *S. aureus*. The BB medium alone or supplemented by silver at the defined concentrations was renewed at 2, 4, 6, 20, 24 and 48 h for *S. aureus* of incubation at 37°C after two gentle rinses with sterile distilled water (2 cm³). Biofilms were grown for 48 hours. After the period of growth the wells were rinsed and 2 cm³ of distilled water were added. Adherent bacteria were removed by scrapping with a sterile spatula and the presence or not of adherent cultivable bacteria was checked by incorporating the solution in trypticase soy agar (Biomérieux) (incubation 48 h at 37°C). Assay was performed in duplicate.

Experiment on cement pellets:

S. aureus CIP 4.83 and *S. epidermidis* CIP 68.21 were grown in 24-well microplates containing pellet of cement with/without silver (the silver concentration ranged from 0.000375% to 3.75% (w/w) of Ag in the cement solid phase) and 2 cm³ of BB. In such conditions, bacteria were in contact with the cement and with the surrounding solution. After initial inoculation with 10² CFU, the adhesion step was considered at 2 h for *S. aureus* and 6 h

for *S. epidermidis*. The BB medium was renewed at 2, 4, 6, 20, 24 and 48 h for *S. aureus* and 6, 20, 24 and 48 h for *S. epidermidis* of incubation at 37°C after two gentle rinses with sterilized distilled water (2 cm³). Biofilms were grown for 72 hours. After the period of growth (72 h), the wells and pellets were rinsed and 2 cm³ of distilled water were added. Adherent bacteria were removed by scrapping with a sterile spatula. Then suspension was homogenized and 10 fold dilutions were performed. One hundred µL of the initial suspension and 1 mL of each dilution were poured in tryptic soy agar (Biomérieux). Plates were incubated at 37°C during 48 h before CFU counting. Results were expressed in log of CFU/mL of recovery solution. Each experiment was performed in triplicate.

2.4. Preparation and rheological characterization of CMC and CMC-Ag solutions

Polymer solutions in water, with CMC concentration ranging from 2 g/L to 10 g/L were obtained by stirring for 30 minutes at room temperature. The rheological behavior of CMC solutions was studied using a controlled stress rheometer (Haake Rheostress RS 75) equipped with a cone plate geometry (6 cm in diameter; 1° angle). Measurements were obtained with imposed shear rate ranging from 0 to 2000 s⁻¹.

According to the target Ag⁺ concentration and the maximum microsphere load in the cement, an Ag⁺ concentration of 0.8 g/L was obtained by dissolving AgNO₃ in the polymer solution used for the preparation of spray-dried silver-loaded microspheres. We first checked that the presence of silver and nitrate ions in the polymer solution did not alter the rheological properties of the polymer solution to be spray-dried.

2.5. Production of CMC and CMC-Ag microspheres using spray-drying process and microparticles characterization

In order to guarantee a high silver loading and homogeneous silver distribution within the CMC microparticles, silver was spray-dried in solution; silver nitrate was preferred as it was fully soluble in the range of CMC solutions studied.

2.5.1. Production of CMC and CMC-Ag microspheres

Microparticles were produced using a Buchi spray dryer model B290 (Buchi, Germany). Briefly, the polymer solution, with CMC concentrations ranging from 2 g/L to 8 g/L and a fully dissolved amount of AgNO₃, was fed into the instrument at controlled rate using a peristaltic pump and sprayed with a 0.7 mm nozzle in the drying chamber of the apparatus, using a flow of compressed air. Heated air aspirated by a pump induced the quick evaporation

of the liquid part of the drops, allowing the formation of solid microparticles. The spray-drying experiments were performed with an inlet temperature of 120 °C, an air flow rate of 410 L/h, a liquid feed rate of 0.23 L/h and an aspirator rate of 90%. The obtained microparticles (μ CMC-Ag), after separation from the exhausted air cyclone, were collected and kept in sealed tubes at ambient temperature prior use.

2.5.2. CMC and CMC-Ag microspheres characterization

The as-synthesized CMC microparticles were characterized in term of morphology, particle size distribution and encapsulation efficiency.

Morphology: Dried microspheres were observed by scanning electron microscopy (SEM) with a LEO 435VP microscope.

Particles size distributions were assessed with a laser particle sizer Mastersizer 2000 (Malvern, UK) based on a laser light scattering technique. Each sample was measured in triplicate. The volume moment mean diameters, $D[4,3]$ and $D(0.5)$ were used to describe the particles size. The polydispersity was evaluated by calculation of samples polydispersity index $PI = [D(0.9) - D(0.1)] / D(0.5)$.

Ag content of microparticles: encapsulation efficiency

The amount of encapsulated silver (Ag^+) per mg of dried microspheres was determined by high-resolution continuum source atomic absorption spectrometry (HR-CS AAS, ContrAA® 300 instrument, Analytik Jena), after complete degradation (i.e. after 72 hours) of 100 mg of microspheres into a Tris buffer 0.1 M pH 7.4 solution under stirring at room temperature. Encapsulation efficiency was calculated by the ratio between this titrated Ag^+ amount to the Ag^+ amount initially incorporated in the polymer solution prior spray-drying. An encapsulation efficiency over 90% was obtained for each batch of Ag-loaded microspheres.

2.6. Preparation of the reference and silver-loaded cements

The reference cement paste was prepared by mixing the appropriate amount of liquid phase (deionized water) with a powder mixture of synthesized brushite (dicalcium phosphate dihydrate: DCPD $CaHPO_4 \cdot 2H_2O$) and vaterite ($CaCO_3$), as previously published [30]. In the present study the powder and liquid phases were mixed using a liquid/solid weight ratio of 0.7 leading to the corresponding reference mineral cement (C-REF'). In view of evaluating the effect of the cement formulation on drug (silver ions) release ability, silver ions were incorporated in the cement powder mixture according to two protocols: by adding synthetic

Ag₃PO₄ powder or AgNO₃-loaded CMC microspheres (μ CMC-Ag) as described above, leading to the C-Ag and C- μ CMC-Ag types of cement, respectively.

For the preliminary *in vitro* anti-biofilm test, we prepared C-Ag cements including different ratios of Ag (from 0.000375% to 3.75 % of Ag (w/w) in the solid phase) to determine the concentration of silver able to impact biofilm formation. For the lowest Ag ratios (*i.e.* 0.000375% and 0.00375% Ag (w/w)) it was too difficult to introduce accurately such a low amount of Ag₃PO₄ powder into the cement formulation; we thus decided to introduce silver *via* the cement liquid phase by using a solution of AgNO₃ which was easily diluted to lower the amount of Ag included in the cement down to 0.000375% Ag (w/w).

For the *in vitro* release study, we formulated both C-Ag and C- μ CMC-Ag types of cement in order to obtain the same weight % of Ag (0.375% Ag (w/w) in the solid phase) introduced either as Ag₃PO₄ powder or as Ag-loaded CMC microspheres, respectively. This silver ratio of 0.375% Ag (w/w) of the solid phase was selected based on the *in vitro* anti-biofilm results for C-Ag cements including different ratios of Ag. In the case of microspheres-loaded cements, the required amount of silver-loaded microspheres (μ CMC-Ag) to reach 0.375% of Ag (w/w) in the solid phase (as in C-Ag) is 10 % (w/w) of the solid phase. Indeed the ratio of Ag in the synthesized microspheres (*i.e.* the loading efficiency) was determined to be 3.75% Ag (w/w). The Ag-loaded microspheres were added to the reference paste after 1 minute of manual mixing. The pastes were then filled into silicone moulds, placed in sealed containers and let at 37°C in a water saturated atmosphere for 48 h, for setting and hardening. Then the set cement pellets were unmoulded and dried at 37°C for two additional days.

In addition, before the biological testing, the surface of each cement pellets (10 mm in diameter) was polished with sand paper (P1200) and gamma sterilized (25 kGy).

2.7. Characterization of cement pastes and hardened blocks

2.7.1. Structural and microstructural characterization

The synthesized powders (DCPD, vaterite and silver phosphate) and the set and dried silver-loaded composite cements was analyzed by X-ray diffraction using a CPS 120 INEL diffractometer with a Co anticathode ($\lambda_{Co} = 1.7903 \text{ \AA}$) and scanning electron microscopy using LEO 435 VP microscope. The total porosity of the composite cements were measured by mercury intrusion porosimetry (Autopore IV 9400 Micromeritics Instruments).

2.7.2. *Injectability and setting time of the cement paste*

The injectability of the C-REF' and C- μ CMC-Ag cement pastes was measured at room temperature using a TAXT2 texture analyzer (Stable Micro Systems) equipped with a specific syringe system, including a 2.5 mL syringe (inner diameter of the syringe body was 9 mm and the opening/exit diameter was 2 mm) without a needle according to a protocol previously published [64]. In addition for C- μ CMC-Ag we tested the potential effect of the amount of μ CMC-Ag microspheres on the injectability of the paste: 2 or 10% (w/w) of μ CMC-Ag were introduced in the cement solid phase. We thus specified the weight ratio in the sample name only for the injectability, total porosity and mechanical properties measurements: C-2 μ CMC-Ag and C-10 μ CMC-Ag, respectively.

The setting time of the cement paste (C-REF' and C- μ CMC-Ag) was evaluated by the Gillmore needle method (standard ISO 9917-1:2007).

2.7.3. *Mechanical properties of the hardened cements*

The reference or composite cement paste was introduced into cylindrical moulds (10 mm in diameter and 20 mm in height), which were then placed in sealed containers saturated with water at 37°C for setting and hardening. After 2 days, the hardened cement was withdrawn from the mould and left to dry for 1 week at 37°C. Five cements were prepared for each of the tested cement formulations. The compressive strength of the cylindrical cement blocks was evaluated using a Hounsfield Series S apparatus.

2.8. *In vitro* release study

2.8.1. *Silver release test*

The release of Ag⁺ from C-Ag and C- μ CMC-Ag cements both including 0.375% of Ag (w/w) in the cement solid phase (as described in 2.6 section) was evaluated using a dissolution USP Paddle Apparatus 2 (Sotax AG, Switzerland). *In vitro* release tests were carried out at 37.0 \pm 0.5 °C with a rotation speed of 100 rpm in 1 L of 0.1 M Tris buffer pH 7.4. The experiments were conducted under sink conditions, as recommended in European Pharmacopoeia guidelines [65]. A block of hardened cement (C-Ag and C- μ CMC-Ag type cement) of about 1.5 g was placed in each vessel. Periodically (from t = 3h to day 13), 15 mL of release medium were collected and replaced by a same volume of fresh Tris buffer in order

to maintain sink conditions. After 13 days, the cements were crushed and a high rotation speed applied during a week in order to determine the maximum (100%) silver able to be released from both cements. The silver released concentration in Tris was determined by high-resolution continuum source atomic absorption spectrometry (HR-CS AAS, ContrAA® 300 instrument, Analytik Jena). The *in vitro* release studies were performed in triplicate for each cement type tested. The % of Ag⁺ released was expressed as:

% Ag⁺ released at T time = amount of Ag⁺ released in dissolution medium (in ppm) at T time / the maximum (100%) silver amount able to be released from the cement in dissolution medium (in ppm) *100.

Tris buffer was chosen as a buffer for this study as it does not contain any calcium or phosphate ions that could influence cement dissolution and/or silver release results.

2.8.2. Silver ions release data analysis

The experimental release data were then fitted to the following semi-empirical equations respectively (i) Higuchi model, which is adapted to solid drugs dispersed in solid granular matrices [66] and diffusion-controlled matrix systems [67], (ii) Weibull model, which is adapted to heterogeneous systems [68] and dissolution release mechanism from microspheres [69].

In Higuchi model, the ratio $Q(t)/Q_0$ between the cumulative percentage of drug released at time t and at infinite time is:

$$Q(t)/Q_0 = K_H \cdot (t - t_{lag})^{1/2} \quad (i)$$

Where K_H is the dissolution constant, coefficient calculated by plotting the linear forms of the Higuchi equation.

In Weibull model, $Q(t)/Q_0$ is:

$$Q(t)/Q_0 = 1 - \exp[-(t - t_{lag})^\beta / t_{scale}] \quad (ii)$$

where t_{scale} is indicative of the time scale for the release process and β characterizes the shape of the release curve.

In both equations, t_{lag} is the lag time before drug release takes place.

The release data up to 80% released silver ions were used to produce theoretical release curves. DDSolver Add-in program [70] was used for modeling and comparing drug release data.

2.9. Statistical analysis

Results are expressed as mean \pm standard deviation. Statistical comparison of the data was performed using the t-test for comparison between two groups or one-way ANOVA and post hoc Bonferroni's test for comparison of more than two groups. A value of $p < 0.05$ was considered significant. For the comparison of silver release profiles, the similarity factor f_2 was estimated according to the International Council for Harmonisation of Technical Requirements for Pharmaceuticals for Human Use (ICH) guidelines.

A summary of the nomenclature of samples and their respective brief description is presented in Table SI.1.

3. Results and discussion

In order to define the range of silver dose to be included in the microspheres to confer to the cement antibacterial properties without cytotoxicity, we first investigated the cytotoxicity and antibacterial activity of two silver salts (Ag_3PO_4 and AgNO_3) exhibiting different solubilities in aqueous solution. These silver salts were used then to formulate the silver-loaded cements, C-Ag and C- μCMC -Ag, respectively. This first step was essential to determine the more appropriate silver salt to add in a cement to preserve silver release properties and optimize cement formulation injectability. Then Ag-loaded microparticles were prepared using a spray-drying process. The process parameters were optimized to obtain silver-loaded microparticles whose characteristics fulfil our requirements in terms of encapsulation efficiency and size, to guarantee antibacterial efficiency and cement injectability, respectively. Then, composite cement formulations with various Ag/CMC/mineral cement ratios have been tested and compared to the reference mineral cement in terms of paste properties, silver release ability and biological properties (cytotoxicity and anti-biofilm properties).

3.1. *In vitro* biological testing of silver salts in solution and C-Ag cements

3.1.1. *Cytotoxicity test*

The cell cytotoxicity results are shown in Figures 1 and 2 for Ag_3PO_4 and AgNO_3 solution samples, respectively. For Ag_3PO_4 solution samples (Figure 1), the non-diluted solution sample (3865 ppm of Ag) had maximum toxicity for hBMSCs with less than 10% live cells

whereas we did not observe toxicity for any of the diluted solutions (1/10, 1/100 and 1/1000 (v/v)). It should be noted that the amount of silver indicated in Figure 1 for each solution samples corresponded to the total amount of silver, *i.e.* silver dissolved in the medium and in the solid particles in suspension. Indeed Ag_3PO_4 salt is a poorly soluble salt in water at 20°C: 6.4 mg.L⁻¹, which corresponds to 4.95 ppm of silver ions. Consequently Ag_3PO_4 partly dissolved in alpha MEM medium (for the non-diluted, the 1/10 and 1/100 (v/v) diluted samples) and some salt particles remained in the solution except for the 1/1000 (v/v) diluted sample. In the latter case the silver ions concentration (3.86 ppm of silver) was under the solubility limit in water for Ag_3PO_4 .

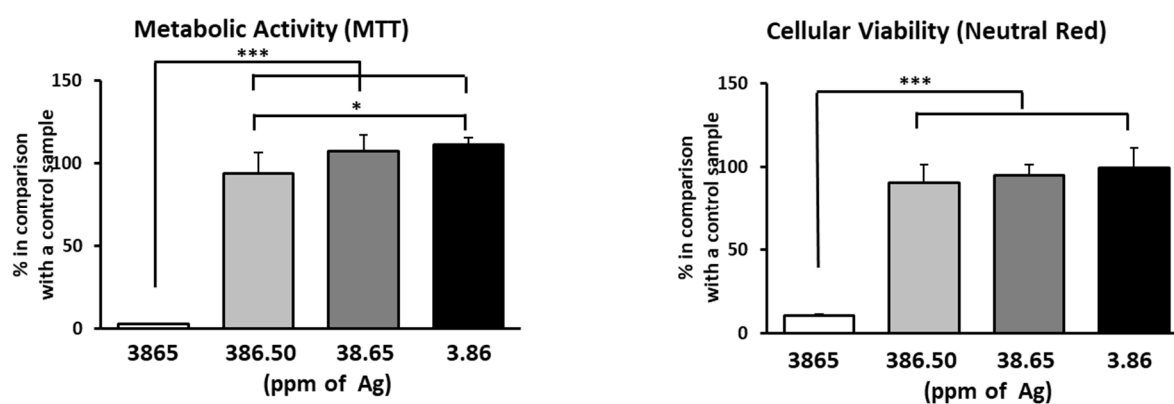


Figure 1: Cell metabolic activity (MTT assay; on the left) and viability (neutral red assay; on the right) of hBMSCs after incubation in alpha MEM containing a different Ag_3PO_4 amount depending on the dilution rate (from 3865 ppm for the non-diluted sample to 3.86 ppm of silver for the 1/1000 (v/v) diluted sample).

Contrary to Ag_3PO_4 , AgNO_3 is a highly soluble silver salt in water (2160 g.L⁻¹ at 20°C) which fully dissolved in alpha MEM in the range of concentrations tested in the present study (Figure 2). We can see that the solution samples were toxic to hBMSCs cells except for the 1/1000 (v/v) diluted solution (3.17 ppm of Ag. With neutral red testing the non-diluted solution (3175 ppm of Ag) was found to be significantly less cytotoxic than the 1/10 and 1/100 (v/v) diluted ones, which seemed inconsistent. However, these three solutions were considered as cytotoxic because their corresponding cell viability was well under the threshold of 70%.

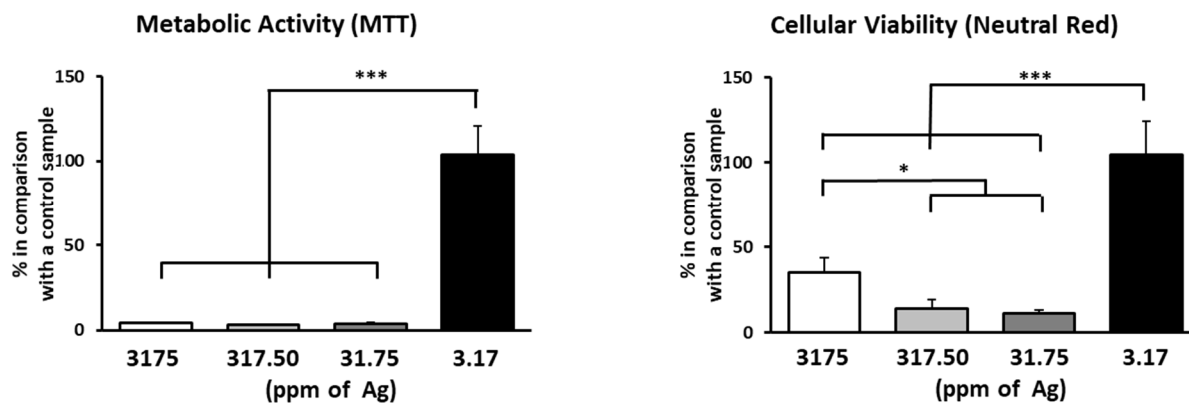


Figure 2: Cell metabolic activity (MTT assay; on the left) and viability (neutral red assay; on the right) of hBMSCs after incubation in alpha MEM containing a different AgNO_3 amount depending on the dilution rate (from 3175 ppm for the non-diluted sample to 3.17 ppm of silver for the 1/1000 (v/v) diluted sample).

These cytotoxicity results on silver salt solution/suspension samples showed that Ag_3PO_4 which is the least soluble salt tested was less cytotoxic than AgNO_3 (fully soluble). The former was found to be non-cytotoxic except for the highest rate tested corresponding to 3865 ppm of silver considering silver both in the medium and in the solid particles. They also showed that cytotoxicity of silver was dependent on whether it was ionized in solution or remained as solid (significant difference of metabolic activity between the 386.50 ppm of Ag and 3.86 ppm of Ag samples, see Figure 1).

Then the antibacterial activity of silver salts solutions has been also evaluated *in vitro* on the selected strains belonging to the main Gram positive species involved in bone and implants associated infections (*S. epidermidis* and *S. aureus*).

3.1.2. Determination of MIC and MBC

The minimal inhibitory concentrations (MIC) and the minimal bactericidal concentrations (MBC) of AgNO_3 and Ag_3PO_4 salts on staphylococci strains were determined; their respective values are reported in Table 1.

Table 1: Minimal inhibitory concentration (in ppm of Ag) and minimal bactericidal concentration (in ppm of Ag) on *S. aureus* CIP 4.83, *S. epidermidis* CIP 6821T, *S. aureus* CRBIP 21.18 (MRSA and multiresistant) and *S. aureus* ATCC 33591 (MRSA) strains of AgNO₃ and Ag₃PO₄ salts in aqueous solution. Assays performed in duplicate.

	AgNO ₃		Ag ₃ PO ₄	
	MIC	MBC	MIC	MBC
<i>S. aureus</i> CIP 4.83	6.3	12.6	0.6	0.6
<i>S. epidermidis</i> CIP 6821T	3.2	6.3	0.3	0.3
<i>S. aureus</i> CRBIP 21.18	6.3	12.6	0.6	0.6
<i>S. aureus</i> ATCC 33591	3.2	6.3	0.3	0.3

Regarding MIC/MBC determination, we confirmed that both salts (silver in the ionic form) are bactericidal agents [17-18] and Ag₃PO₄ appeared more active than AgNO₃ *in contrario* to the results from cytotoxicity assays (Figures 1 and 2). Experimental aspects can be brought into play: the media were very different which may have an impact on each salt behavior (solubility) and availability, and mode of action for very different cell types (bacteria and hBMSCs). On the other hand, cytotoxicity tests were carried out directly on confluent cells whereas the antibacterial activity tests were carried out by adding the salts from t₀, before the beginning of the cell growth phase.

Considering the cytotoxicity and antibacterial activity of both silver salts (Figures 1 and 2 and Table 1), it appeared that Ag₃PO₄ showed the larger range of silver concentrations able to confer antibacterial properties without being cytotoxic. This is the reason why the anti-biofilm study (Table 2) was performed with Ag₃PO₄ salt and Figure 3 established based on Ag₃PO₄ biological properties results. Anti-biofilm activity of Ag₃PO₄ was evaluated against *S. aureus* CIP 4.83 by adding this salt at t₀ while inoculation, or 2 h after the inoculation. The added concentrations expressed in silver were 0.0025 ppm, 0.025 ppm, 0.25 ppm and 2.5 ppm. Biofilm formation was checked after 48 h of incubation (detection or not of adherent cultivable bacteria). In such conditions (Table 2), the lowest tested concentration (0.0025 ppm) had no anti-biofilm activity in both conditions (addition at t₀ or t_{2h}). A total anti-biofilm activity was noted for the two highest concentrations: 2.5 and 0.25 ppm. The silver concentration 0.025 ppm permits a total inhibition of biofilm formation when added at t₀ but when added 2 h after the inoculation, which may be considered for the adhesion step, this concentration was not able to prevent biofilm formation. It could be considered that 0.025

ppm of silver were able to impair *S. aureus* adhesion but not their proliferation under biofilm after adhesion.

Table 2: Anti-biofilm activity of Ag_3PO_4 in aqueous solution (in ppm of Ag) on *S. aureus* CIP 4.83 when addition was performed at t_0 with inoculation or 2h after inoculation (t_{2h}). Control performed without any silver addition. (+): detection of cultivable adherent bacteria; (-): no detection of cultivable adherent bacteria. Assays performed in duplicate.

Ag concentration (ppm)	Addition at t_0	Addition at t_{2h}
2.5	-	-
0.25	-	-
0.025	-	+
0.0025	+	+
Control	+	+

The microbiological and cytotoxicity results on Ag_3PO_4 allowed to determine the target range corresponding to the range of silver ions concentration conferring anti-biofilm properties without being cytotoxic: between 0.025 and 4.95 ppm of silver (Figure 3, blue double arrow delimited zone).

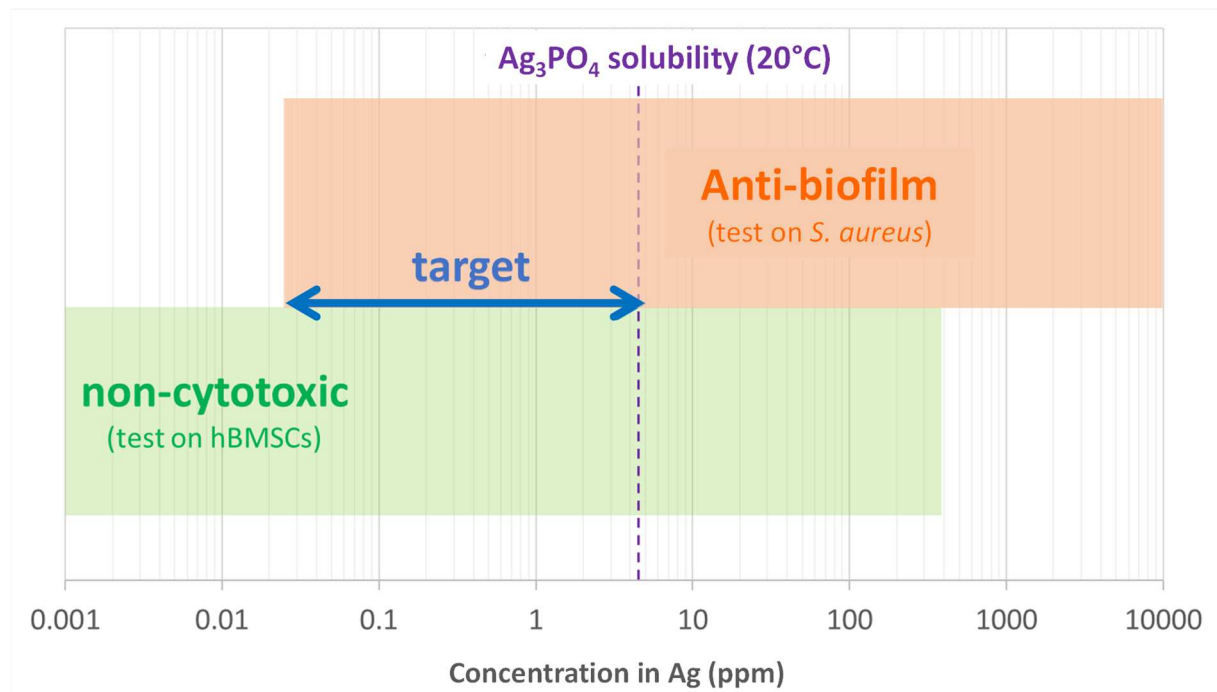


Figure 3: Concentration of silver as Ag_3PO_4 salt in solution (in ppm of Ag) with regard to its non-cytotoxicity (green range: test on hBMSCs) and anti-biofilm properties on *S. aureus* strain (orange range). Range of silver concentrations being antibacterial but not cytotoxic indicated as the targeted Ag concentration range (addition at t_0) delimited by the blue double

arrow. The solubility of Ag_3PO_4 salt at 20°C expressed as silver concentration is also reported on this figure (purple dashed line).

After having evaluated the cytotoxicity and bactericidal concentration (*S. aureus* CIP 4.83 and *S. epidermidis* CIP 6821T) of two silver salts of a very different solubility in aqueous solution, and anti-biofilm concentration of Ag_3PO_4 on *S. aureus* CIP 4.83, the anti-biofilm properties of C-Ag cements including a different Ag_3PO_4 amount in the cement solid phase were evaluated *in vitro*.

It should be noted that the concentration of Ag in cement solid phase should not be directly correlated to the silver concentration in solution/suspension considered for microbiological and cytotoxicity tests. Indeed when in apatitic cement the silver either included in CMC microspheres or not is not fully available as it could be in Ag_3PO_4 or AgNO_3 aqueous solutions/suspensions.

3.1.3. *In vitro* anti-biofilm properties of C-Ag cements

Table 3 presents the CFU values on C-REF' and C-Ag cement pellets after 72 h of incubation for *S. aureus* CIP 4.83 and *S. epidermidis* CIP 68.21. For both tested bacteria which represent the main species involved in bone-implant infection, the antibacterial efficiency was significant from 0.0375% (w/w) silver-loading in the cement formulation. This anti-biofilm formation effect was significant whatever the silver salt considered. However the difference between Ag_3PO_4 -loaded and AgNO_3 -loaded cements was also significant ($p < 0.001$) for the 0.0375% Ag (w/w) cements (Table 3): the Ag_3PO_4 -loaded cement showed higher antibacterial activity on both strains than the AgNO_3 -loaded one. It is noteworthy to mention that although the silver salts were not the same, a same amount in ppm of Ag was used in the cement for comparison. Indeed due to the difficulty to introduce very low amount of silver as Ag_3PO_4 powder to prepare the 0.00375% and 0.000375% Ag (w/w) cement formulations, we used a AgNO_3 solution which can be easily diluted to prepare these two cements (C-Ag 0.00375% and C-Ag 0.000375%) and also the 0.0375% Ag (w/w) one (C-Ag 0.0375%**; Table 3) to compare with the one loaded with Ag_3PO_4 (C-Ag 0.0375%*, Table 3).

Table 3: Numeration (log CFU/mL) of adherent bacteria (*S. aureus* CIP 4.83 and *S. epidermidis* CIP 68.21) after 72 h of incubation with pellet of the reference mineral cement (C-REF': control without silver) or C-Ag cements containing various concentrations of silver (from 0.000375% up to 3.75% Ag (w/w)) introduced as Ag₃PO₄ in the solid phase (*) or as AgNO₃ in the liquid phase (**) for the lowest concentrations (mean ± SD; n = 3). NS: non-significant.

	C-Ag 3.75%*	C-Ag 0.375%*	C-Ag 0.0375%*	C-Ag 0.0375%**	C-Ag 0.00375%**	C-Ag 0.000375%**	C-REF' (Control)
<i>S. aureus</i> CIP 4.83	< 3	< 3	< 3	4.29 ± 0.23	6.84 ± 0.10	6.69 ± 0.34	6.98 ± 0.12
p-value (control vs assay)	< 0.001	< 0.001	< 0.001	< 0.001	NS	NS	
<i>S. epidermidis</i> CIP 68.21	< 3	< 3	< 3	4.56 ± 0.06	6.82 ± 0.04	6.47 ± 0.25	6.86 ± 0.04
p-value (control vs assay)	< 0.001	< 0.001	< 0.001	< 0.001	NS	NS	

A previous study of Jacquart *et al.* [30] showed that a cement loaded with a much higher silver concentration (7.5% Ag (w/w)) whether as Ag₃PO₄ in the solid phase or AgNO₃ in the liquid phase of the cement formulation, was non-cytotoxic. Considering the present anti-biofilm test results for C-Ag cement formulations with different silver concentrations, we then focused on the optimum silver loading concentrations (0.375 and 0.0375% Ag (w/w) in the cement solid phase) able to confer anti-biofilm properties and non-cytotoxicity to formulate injectable silver-loaded composite cements.

Our goal was to obtain microspheres small enough to preserve paste injectability when added in the cement, *i.e.* of about 5 to 30 µm in diameter, together with the best yield of silver encapsulation. For this purpose, a spray-drying process was chosen. In comparison with solvent evaporation after emulsification, a competitor method to produce microspheres, spray-drying results in a one-pot synthesis, avoiding time-consuming steps and the use of harsh solvents [71]. It is compatible with on-line continuous production and can be easily scaled up, a necessity for further industrial development.

The production of CMC microspheres by spray-drying has already been reported in the literature [57], but the operating conditions can affect particle size and morphology. The

presence of an active compound (Ag^+) in solution may also have an influence as it could modify in an unpredictable manner the viscosity of the solution to spray-dry. Thus the physico-chemical characteristics of the silver salt, in particular its solubility, play a crucial role on the encapsulation efficiency value. To guarantee homogeneous silver distribution within the microparticles, AgNO_3 amounts fully dissolved in CMC solution were used. Silver ions may interfere with polymeric chains, modifying their conformation and possibly hindering their gelation properties. As a consequence, we first studied the influence of CMC and silver concentrations in solution on the resulting microspheres.

3.2. Optimization of the operating conditions of the spray-drying process and resulting microspheres characterization

Various parameters may influence microspheres morphology and process yield. Some are directly correlated to the process parameters: atomizing gas flow rate, drying gas flow rate, feedstock flow rate, inlet temperature [72] (see the instrumental settings used in the present study in the 2.5.1 section for). Others depend on the properties of the spray-dried solutions. In order to determine the best operating conditions, CMC solutions of concentration ranging from 1 to 10 g/L have been characterized with a rheometer before being spray-dried. The morphology and the size distribution of the resulting microspheres, according to the viscosity of CMC solutions, are presented in Figure 4.

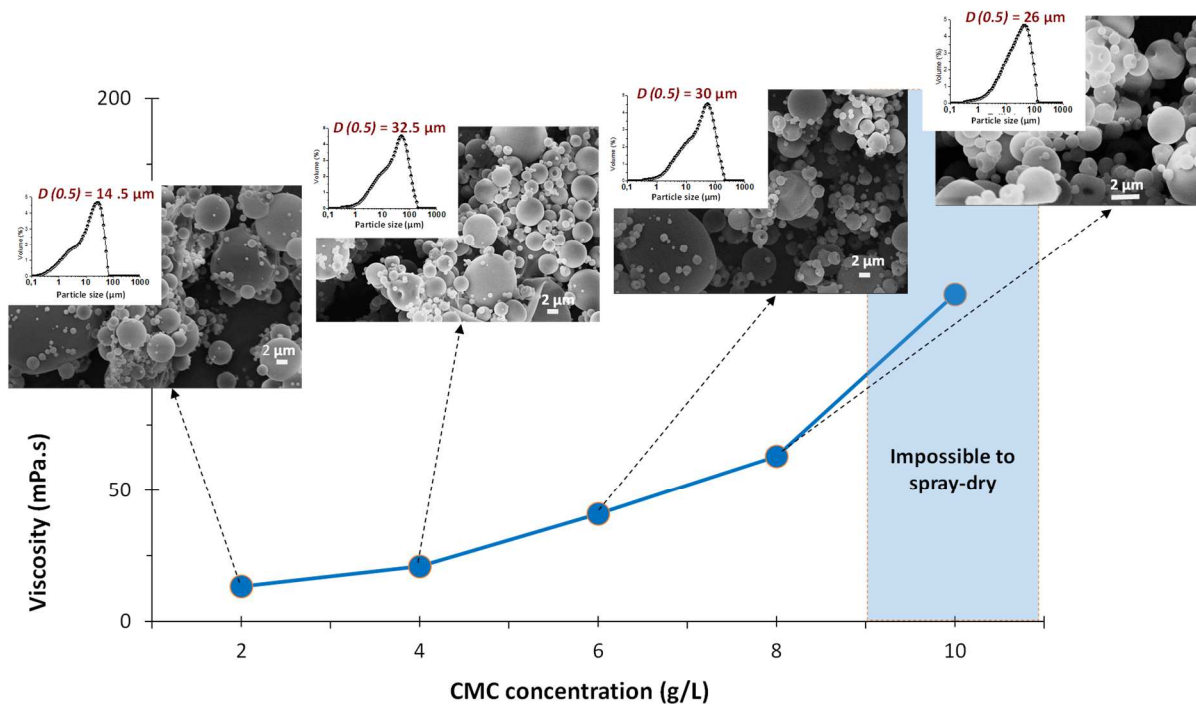


Figure 4: Viscosity of CMC solutions as a function of CMC concentration, measured at a shear rate of 1000 s^{-1} . SEM micrographs and particle size distribution of corresponding spray-dried CMC microspheres are presented at the top of the figure.

For all the CMC concentrations tested, the solutions exhibited a shear-thinning, non-thixotropic, behavior. A concentration of 2 g/L was determined as the minimum threshold of concentration to obtain microspheres, and a concentration of 10 g/L resulted in too viscous solutions. Between these limits the obtained microspheres appeared spherical and smooth (Figure 4). Increasing polymer concentration increased particle sizes by a combination of i) a decrease of the ratio of small particles, which are more difficult to collect and ii) an increase of viscosity, both impacting the polydispersity index (PI) of the batches. These results were coherent with previously published studies with other biopolymers such as hyaluronic acid [36] or chitosan [73].

The viscosities were measured for various concentrations of CMC, in presence or absence of silver ions in solution (Figure SI.2, left side). No variation in viscosity was observed until CMC concentration reached 8 g/L. In addition, no significant difference in particle size distribution was noticed in presence or absence of silver salt in a 4 g/L CMC solution (Figure SI.2 right side and middle). As a consequence, a CMC concentration of 4 g/L was chosen as operating condition for the following silver-loaded CMC microspheres synthesis. These

conditions permitted to obtain CMC microspheres in a reproducible manner, with polydispersity indexes lower than 3 (Table 4).

Table 4: Characteristics of the CMC solutions and of the resulting spray-dried microparticles: viscosity of the CMC solutions (4 g/L of CMC with or without AgNO₃) prior spray-drying at 1000 s⁻¹ (mPa.s); D(0.5), D[4,3] and polydispersity index (PI) of CMC and silver-loaded CMC microparticles; silver loading of silver-loaded CMC microparticles.

	CMC solutions and microparticles	
	CMC only	CMC + AgNO ₃ (0.8 g/L)
Viscosity of the CMC solution prior spray-drying at 1000 s⁻¹ (mPa.s)	20.9 ± 3.2	25.1 ± 2.6
D(0.5)	32.9 ± 4.1 μm	29.2 ± 6.0 μm
D[4,3]	39.0 ± 5.1 μm	40.0 ± 1.3 μm
PI	2.3 ± 0.1	2.5 ± 0.2
Silver loading (g of Ag / g of microspheres)	-	0.0375

Concerning the microspheres incorporated in the C-μCMC-Ag cement for the release study, a silver loading of 0.0375 g/g of microspheres was obtained, with a high encapsulation efficiency (> 90%).

Once synthesized, the silver-loaded CMC microparticles (μCMC-Ag) have been introduced in the cement formulation and the anti-biofilm and physical-chemical properties of the cement studied.

3.3. Biological and release properties of Ag-loaded CMC microspheres composite cements

3.3.1. *In vitro* anti-biofilm properties of C-μCMC-Ag cements

The anti-biofilm properties of the C-μCMC-Ag cement were evaluated on *S. aureus* strain (Table 5) and compared with those of the reference mineral cement as control (C-REF³); a reference composite cement with CMC raw powder (10% (w/w)) but no silver (C-pCMC) was also tested. Due to the slightly lower anti-bacterial activity already observed (C-Ag cements, Table 3) for 0.0375% Ag (w/w) AgNO₃-loaded cement compared to the Ag₃PO₄-loaded one, the silver load threshold needed to be double checked: thus, we tested both the 0.375 and 0.0375% Ag (w/w) composite cement formulations (C-μCMC-Ag, Table 5). We found that both C-μCMC-Ag formulations tested showed significant anti-biofilm efficiency of about the

same level than that of C-Ag cements (Table 3) and a silver dose effect was also observed. The comparison with the C-pCMC reference composite cement demonstrated that the antibiofilm properties of the C- μ CMC-Ag composites were related to the presence of silver only.

Table 5: Numeration (log CFU/mL) of adherent bacteria (*S. aureus* CIP 4.83) after 72 h of incubation with the cement pellet without silver (control: C-REF'), CMC-containing cement pellet without silver (C-pCMC) or silver-loaded CMC microspheres cement pellet including two concentrations of silver (0.375 and 0.0375 % Ag (w/w) of the C- μ CMC-Ag solid phase) (mean \pm SD; n = 3). Comparison to C-REF'; NS: non-significant.

	C-μCMC-Ag 0.375% Ag (w/w)	C-μCMC-Ag 0.0375% Ag (w/w)	C-pCMC	C-REF' (Control)
<i>S. aureus</i> CIP 4.83	2.34 \pm 0.12	3.15 \pm 0.23	6.78 \pm 0.20	6.71 \pm 0.17
p-value (control vs assay)	0.04	0.04	NS	

Based on the microbiological results on silver salts (Figures 1, 2 and 3) and a previous study of Jacquart *et al.* [30] on mineral cement including (7.5% Ag (w/w) introduced whether as Ag₃PO₄ or AgNO₃), we expected that C- μ CMC-Ag composite cement including 0.375% Ag (w/w) was non-cytotoxic: it was confirmed by *in vitro* cell testing with hBMSCs (Figure SI.3).

We thus chose to introduce 0.375% Ag (w/w) in the mineral (C-Ag) and composite (C- μ CMC-Ag) cements to be tested for the *in vitro* Ag-release study. This choice of Ag-loading was around the optimum silver loading but higher than the 0.0375% Ag threshold able to confer antibiofilm activity, as defined for C-Ag mineral cements (Table 3) and C- μ CMC-Ag composite cements (Table 5). This silver loading (0.375% Ag (w/w) in the solid phase) should allow reaching the target Ag dose range earlier. Indeed the evaluation of silver release was performed to demonstrate the early availability of active dose of embedded silver in view of providing protection of the implant for the time needed to win the “race to the surface,” i.e., in the first hours after surgery.

3.3.2. *In vitro* release of silver from CMC microspheres loaded cements (C- μ CMC-Ag) and from Ag_3PO_4 -loaded cement (C-Ag)

As indicated in 2.6 and 2.8.1 sections, the release of Ag^+ from C-Ag and C- μ CMC-Ag cements was performed on both cement formulations including 0.375% (w/w) of Ag in the cement solid phase, introduced either as Ag_3PO_4 powder (C-Ag mineral cement) or as Ag-loaded CMC microspheres (10% (w/w) of μ CMC-Ag introduced in the cement formulation: C- μ CMC-Ag composite cement). Results of the *in vitro* silver release from C- μ CMC-Ag and C-Ag cements at 37°C in Tris buffer at pH 7.4 are presented in Figure 5. For the comparison of release profiles, the similarity factor f_2 (according ICH guidelines) was estimated. Microspheres-loaded- and reference cements led to significantly different release profiles: similarity factor $f_2 = 23\%$, *i.e.* $< 50\%$, demonstrating that the considered release kinetics can't be considered as similar. Both materials (C-Ag and C- μ CMC-Ag) exhibited release profiles extended on 5 days (in the case of C- μ CMC-Ag) or more, without burst and correspond to a low % of release during the first 3 hours. Then, the silver release rate from C-Ag cement remained significantly slower than that of C- μ CMC-Ag. For the latter, a plateau at 90-100% was reached after 5 days, while only 60% of silver was delivered after 12 days in the case of the C-Ag cement. In all cases the maximum silver released concentration (0.6 ± 0.1 ppm for C- μ CMC-Ag composite cement and 1.03 ± 0.04 ppm for C-Ag mineral cement) was in the targeted silver concentration range as defined in Figure 3. In addition for the C- μ CMC-Ag composite cement this targeted silver dose range was reached within the first hours of release test (0.04 ppm of Ag released at $t = 3\text{h}$) whereas it took one day for the C-Ag mineral cement.

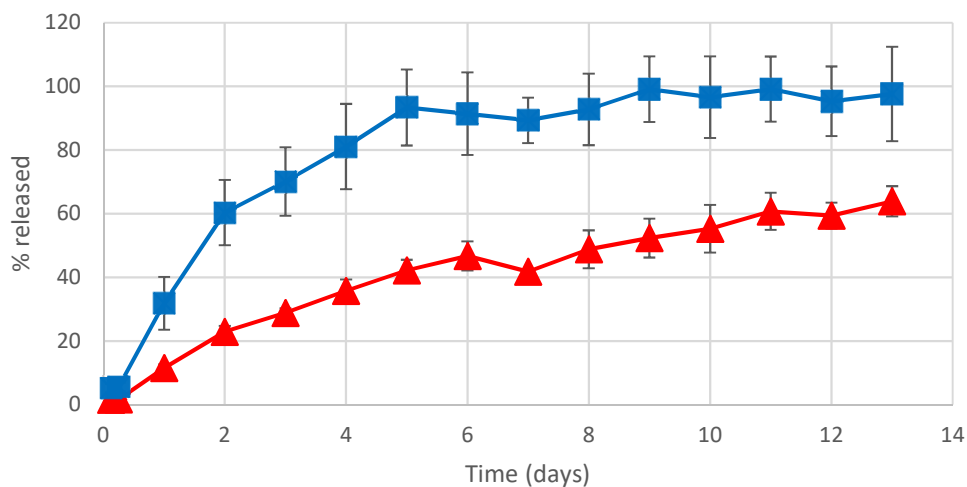


Figure 5: Silver release curves for C-Ag (red triangles) and C- μ CMC-Ag (blue squares) cements both including 0.375% (w/w) Ag in the cement solid phase, introduced as Ag_3PO_4 powder (C-Ag) or as Ag-loaded CMC microspheres (C- μ CMC-Ag), as a function of time over 2 weeks. Silver release is expressed as the % of Ag released compared to the initial amount of silver introduced in the self-setting cement/composite.

The resulting kinetic parameters estimated from Higuchi and Weibull models (see Experimental) are presented in Table 6 to further elucidate the release mechanism.

Table 6: Silver release kinetic parameters estimated from Higuchi and Weibull models for C-Ag and C- μ CMC-Ag cements, with t_{lag} in hours.

Sample	C -Ag cement				C- μ CMC-Ag cement			
	r^2	K_H	t_{lag}	β	r^2	K_H	t_{lag}	β
Higuchi :								
Simple	0.925	3.5			0.950	8.2		
With lagtime	0.995	4	16.1		0.990	8.7	5.6	
Weibull								
	0.997		2.1	0.9	0.994		0.4	1.1

The mathematical analysis of the data confirmed that silver release mechanism was not the same when silver is incorporated directly within the cement and when silver is encapsulated in CMC microspheres prior addition in the mineral cement. Both systems show releases that do not perfectly match with a simple Higuchi model but correlation is highly increased with the Higuchi model with a lag time ($r^2 \approx 0.995$ and 0.990) lowered from 16 h to 5.6 h when silver is loaded in CMC microspheres. The close release profiles during the first 3 hours of a very low amount of Ag may be related to the Ag release from equivalent surfaces of both cements.

Considering the Weibull model, the dependency between its β value and the release mechanism of substances has been established by several authors [36, 68, 74]. Fickian diffusion was estimated for processes with $\beta \leq 0.75$. In β range between 0.75 and 1.0, the Fickian diffusion is combined with case II transport. For β value higher than 1.0, a complex mechanism of drug transport has been reported. The β value obtained for the mineral cement corresponds to a Fickian diffusion combined with a case II transport, and is in accordance with Higuchi modelization results. In the case of composite cements, the β Weibull is in favor of a

more complex release mechanism. Microspheres hydration, cement chemical setting reaction in presence of silver and an hydrophilic polymer, cement and composite porosity are all parameters likely to influence the kinetics of silver release. They will be discussed in the 3.5 section

3.4 Injectability of C-2 μ CMC-Ag and C-10 μ CMC-Ag cement pastes

In addition to the control of local silver delivery at the desired dose, the other main aim pursued was to improve cement injectability in view of minimizing the IAIs risks by using mini-invasive technique of implantation. In this context, we evaluated the effect of the introduction of Ag-loaded CMC microparticles in the cement formulation on the injectability of the composite paste. The extrusion of the composite cement pastes including 2 or 10% (w/w) of Ag-loaded CMC microspheres (C-2 μ CMC-Ag and C-10 μ CMC-Ag cement paste, respectively) was compared to that of the reference mineral cement (C-REF'). The curves of the load as a function of the piston position (piston was displaced at a constant rate, 2 mm/s) are presented on Figure 6. We can see that a filter-pressing phenomenon occurred during C-REF' paste extrusion leading to its poor injectability; indeed the load needed to extrude the volume of paste at a constant rate increased exponentially by up to 26 Kg after 15 mm of piston displacement. Interestingly, this load was reduced down to 6 Kg to extrude the C-2 μ CMC-Ag composite cement paste and to 4 Kg for the C-10 μ CMC-Ag one. In addition the curves for both composite cements (C-2 μ CMC-Ag and C-10 μ CMC-Ag) remained flat after 1 s (2 mm of piston displacement) of paste extrusion and the corresponding loads were well under the accepted limit of manual injectability (12 Kg). These results showed that the C-2 μ CMC-Ag and C-10 μ CMC-Ag composite pastes were injectable and that the introduction of drug delivery systems such as μ CMC-Ag in the cement formulation drastically improved the injectability of these composite cement pastes. The C-10 μ CMC-Ag cement appears as a promising formulation for injectable and antibacterial bone cement applications.

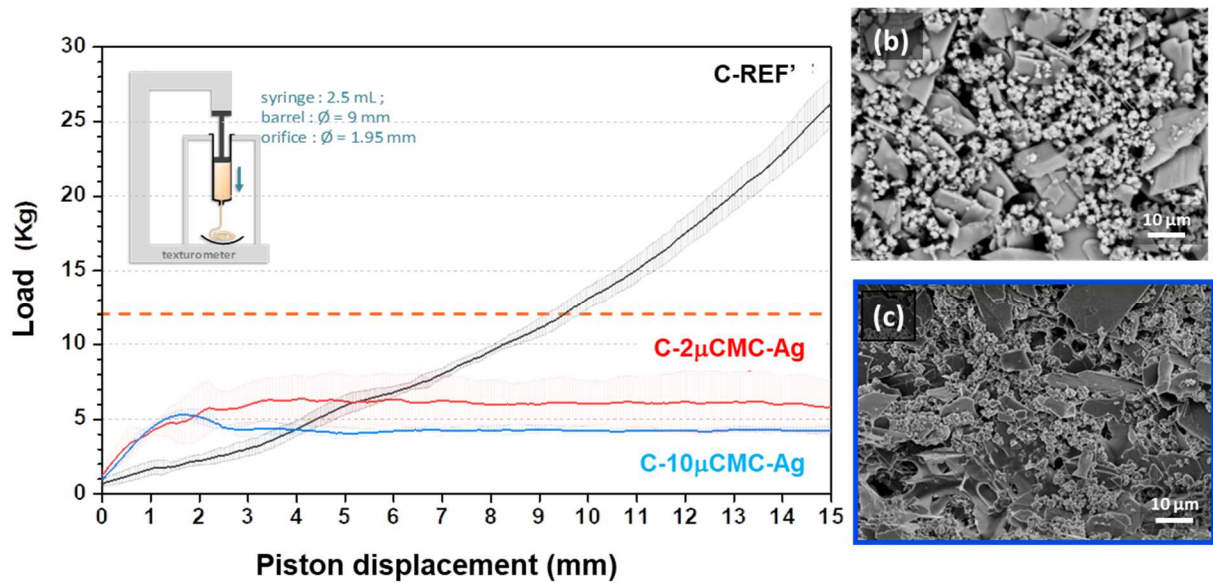


Figure 6: Effect of the introduction of 2 or 10% (w/w) of Ag-loaded CMC microspheres in the cement formulation (C-2 μ CMC-Ag and C-10 μ CMC-Ag, respectively) on the injectability of the cement paste (measured as the load needed to displace the syringe piston at a constant rate) compared with that of the reference mineral cement (C-REF'). SEM micrograph of the extruded paste of the reference cement, C-REF' (b) and C-10 μ CMC-Ag composite cement (c), both lyophilized after extrusion.

To further understand the role of the presence of the CMC microparticles in the cement formulation on the elimination of the phase separation (filter-pressing) phenomenon upon paste extrusion, we performed an additional experiment. We collected and immediately lyophilized the extruded paste after 1h of setting and then observed the dried extrudates of the C-REF' and C-10 μ CMC-Ag by SEM (Figure 6b and 6c, respectively) to examine their microstructure. We observed how the suspension consisting of brushite (platelets), vaterite (spheroids) crystals/particles and CMC microparticles (μ CMC-Ag) was structured when extruded (Figure 6c). Preferential orientation of brushite platelet crystals parallel to the direction of the paste extrusion are clearly visible; this orientation is much more pronounced for the composite paste (Figure 6c) where we can observe the main surface of brushite platelets compared with C-REF' (Figure 6b) for which the brushite platelet crystals showed different orientations (not only horizontal). In addition, the presence of the CMC in the C- μ CMC-Ag composite paste appeared as a binding agent between the reactive particles/crystals (Figure 6c) which contributed in the improvement of the paste cohesiveness: in Figure 6b, the particles in C-REF' paste appeared more individualized compared with the

continuous network of particles/CMC in Figure 6c. However the filter-pressing phenomenon has to be examined deeply to understand the role of CMC. The duality between the increased friction between the reactive particles when the liquid/solid ratio decreases upon extrusion and the filtration phenomenon which is enhanced by the crystals/particles orientation during extrusion to favor the water to pass in between has been reported in the case of construction cement [75]. In the present study, the CMC could have also an effect on different parameters. CMC is an hydrophilic polysaccharide which swelled in the presence of water leading to an increase of the paste volume for a given amount of particles limiting the friction between each other. In addition this phenomenon should also be enhanced by the effect of the steric and electrostatic repulsion between polymer chains wrapping the reactive mineral particles [76] increasing the interparticles space and the effect of the water which is associated to CMC and thus less free to flow in between the reactive particles, thus limiting the filter-pressing phenomenon. Altogether these considerations contribute in understanding the beneficial effect of the presence of CMC in the cement paste injectability.

As the release study was performed on set and hardened Ag-loaded cements, we also investigated the microstructural characteristics and mechanical properties of these composite cements.

3.5. Composite cements composition and microstructure

In order to better understand how parameters such as microspheres hydration, cement chemical setting reaction in presence of silver and hydrophilic polymer, cement and composite porosity can influence silver release, we thoroughly studied composite cement composition and microstructure.

As already shown by Jacquart *et al.* the introduction of silver as Ag_3PO_4 powder in the cement solid phase did not modify significantly the initial setting time ($1\text{h}15 \pm 0\text{h}05$ for C-Ag and $1\text{h}18 \pm 0\text{h}03$ for C-REF') [30]. However the introduction of silver in cement formulation in the form of 10% (w/w) $\mu\text{CMC-Ag}$ delayed it ($1\text{h}45 \pm 0\text{h}15$) but this setting time can be easily adjusted by using a Na_2HPO_4 solution instead of water as the liquid phase to prepare the paste. For example, C- $\mu\text{CMC-Ag}$ setting time was reduced down to $0\text{h}18 \pm 0\text{h}03$ using 1% w/w Na_2HPO_4 solution as liquid phase.

The composition and microstructure of the C-Ag and C- $\mu\text{CMC-Ag}$ cements were characterized before and after the release experiment. By XRD analysis, we found that, before the test, C- $\mu\text{CMC-Ag}$ composite cement was composed of two crystalline phases: apatite and some

unreacted vaterite (Figure 7). After the release test only some very low intensity vaterite peaks (at $2\theta = 29^\circ$, 32° and 52°) remained poorly visible, showing that vaterite almost fully dissolved during this *in vitro* experiment. A peak broadening of the two main diffraction lines of apatite ((002) and (310) line around 31° and 37° , respectively) testified for the presence of a nanocrystalline apatite. Thus after two weeks of immersion in Tris buffer solution, the C- μ CMC-Ag cement was mainly composed of nanocrystalline apatite analogous to bone mineral (Figure 7). We do not present the XRD patterns for C-Ag cement before and after release experiment as they were found to be similar to those of C- μ CMC-Ag, the Ag_3PO_4 crystalline phase being at too low concentration in C-Ag (0.375% of Ag (w/w) in the solid phase) to be detected by XRD.

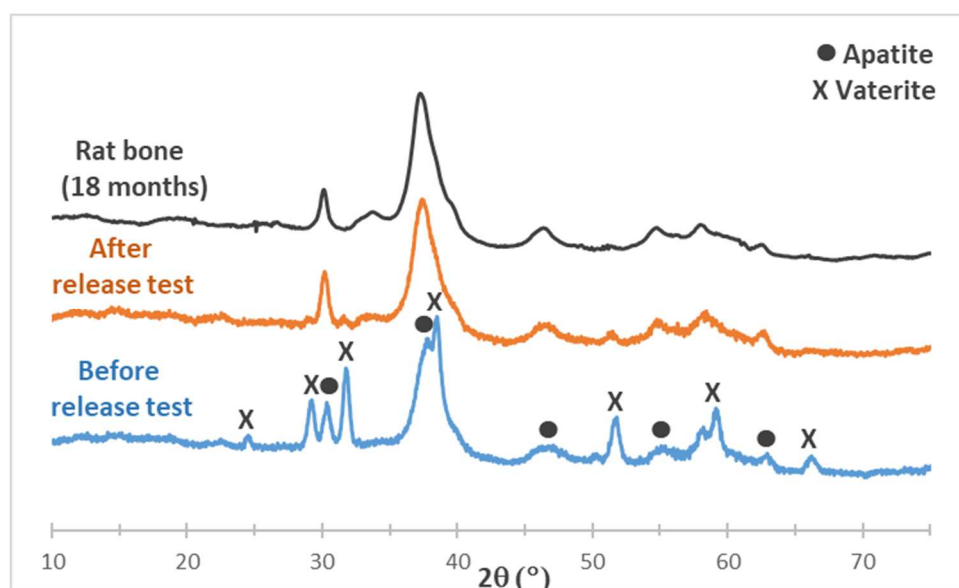


Figure 7: XRD pattern of the C-10 μ CMC-Ag cement before and after 15 days of release test compare with that of rat bone (18 months).

Figure 8 shows the microstructure of the C- μ CMC-Ag composite cement before and after the release test. After the release test microspheres of CMC-Ag were not observed but some hydrogel structures appeared embedded in the mineral cement matrix (Figures 8a, 8b, 8c and 8e). This can be explained by the stability alone upon rehydration of CMC microspheres (data not shown). Indeed when immersed in Tris buffer at pH 7.4, their rehydration profile consisted in a rapid liquid absorption (+2400 % swelling) within the first 2 minutes followed by a plateau and a progressive loss of weight due to microspheres disintegration. After 30 hours, CMC microspheres has become a loose gel; this could explain that no well-defined CMC microparticles can be distinguished on SEM micrographs of C- μ CMC-Ag cement

(Figure 8). Before the release test, both on the backscattered and secondary electron modes micrographs (Figures 8b and 8c) a few brighter small particles are clearly associated to the surface of the CMC layered structure, testifying for the presence of silver rich particles which could correspond to silver or Ag_3PO_4 particles [77]. After the release test, these small brighter particles were no more visible (Figures 8d, 8e and 8f) in agreement with the nearly full release of silver from the C- $\mu\text{CMC-Ag}$ composite cement observed at the end of the release test (Figure 5). Indeed Figures 8d and 8e showed area with CMC embedded in the mineral matrix but no more associated with brighter spots and at higher magnification (Figure 8f) an homogeneous microstructure of the composite cement (without any brighter spots) can be observed.

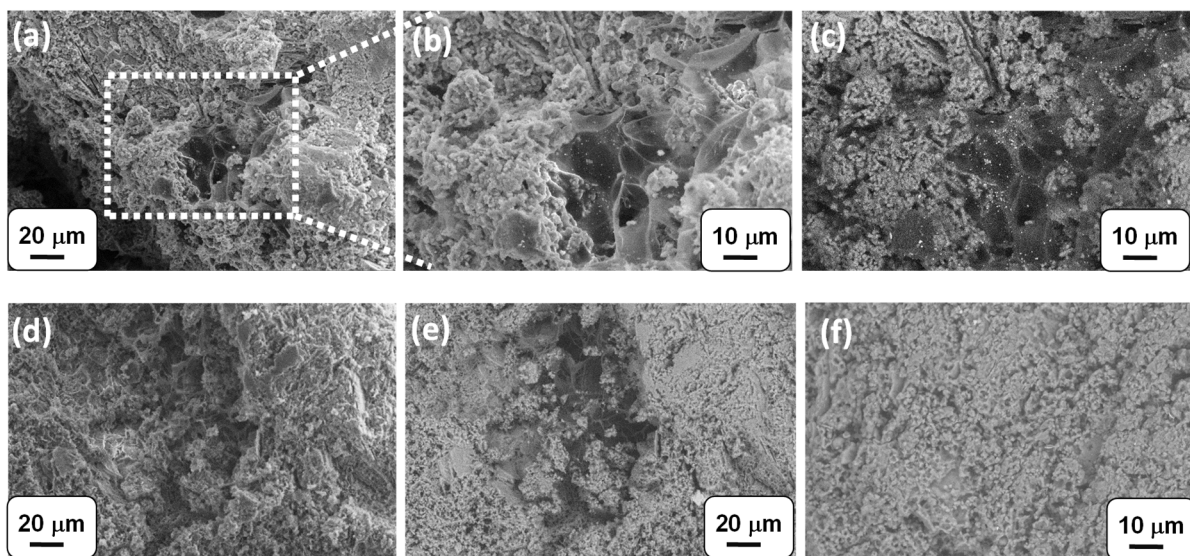


Figure 8: SEM micrographs of the C- $\mu\text{CMC-Ag}$ composite cement before (a, b and c) and after (d, e and f) the release test (13 days at 37°C in Tris buffer). SEM micrographs in secondary electron mode (a, b and d) and in backscattered electron mode (c, e and f); c) corresponds to b) SEM micrograph and e) to the d) one.

The total porosity and compressive strength of the set and hardened C- $\mu\text{CMC-Ag}$ composite cement including 2 or 10% (w/w) of silver-loaded microspheres have been evaluated.

We observed that the introduction of CMC microspheres lowered the cement porosity from 88% for C-REF' down to 77% and 68% for C-10 $\mu\text{CMC-Ag}$ and C-2 $\mu\text{CMC-Ag}$ composite cements, respectively. This can be attributed to the presence of CMC loose gel which clogs the pores of the mineral matrix. However, as it can be seen on the SEM micrographs (Figure 8), the structure of composite cements is not homogeneous, but made up of mineral zones and

organic zones playing the role of silver reservoir. In the case of C-Ag cement, as silver ions are positively charged, they could ionically interact with the mineral phase of the cement during the dissolution-precipitation reactions involved during the cement setting reaction. As a consequence, silver ability to be released in the tissues surrounding the implantation site should be partly prevented, or at least slowed down, even more as Ag_3PO_4 is less soluble than AgNO_3 . On the contrary, encapsulating silver ions into microspheres prior loading in the mineral matrix turns out to be advantageous for a faster silver release, as shown by the increased K_H in the Higuchi simulation, and the decreased t_{lag} in the Higuchi with lagtime and Weibull simulations in the case of C- μCMC -Ag composite (Table 6). Our preliminary experiment on anti-biofilm activity of Ag_3PO_4 solution on *S. aureus* CIP 4.83 (Table 2) well underlined the importance to have sufficient directly available silver to impair the adhesion step then biofilm formation. In view of these modelling results (Table 6, Figure 5), we hypothesize that silver release from microspheres-loaded cement can be considered as a combination of phenomenon related to microspheres hydration, lowered silver interaction on cement setting (final crystalline composition) and composite structure (combining porous mineral parts and loose gelled polysaccharidic parts). Silver faster release might result of the presence of CMC increasing the hydrophilic nature of the cement and consequently the water attraction within the C- μCMC -Ag composite, combined with composite heterogeneity facilitating the outflow of silver in comparison with a conventional mineral cement (C-Ag).

3.6 Cement mechanical properties

The introduction of CMC microspheres in cement formulation had also an effect on others characteristics of the composite cement. The compressive strength of the cements decreased from 12.7 ± 2.7 MPa for C-REF' cement to 5.4 ± 0.5 MPa for C-10 μCMC -Ag composite. This effect was more pronounced especially when CMC microspheres amount was low (2%: C-2 μCMC -Ag composite): 3.5 ± 0.4 MPa. The heterogeneity associated to the introduction of a low amount of a new organic phase (CMC microspheres) in the cement matrix should favor the initiation and propagation of cracks compared with the reference cement. A previous study showed that the CMC powder content threshold to enhance the mechanical properties of C-pCMC composite materials was around 10–20 % thanks to the formation of a polysaccharide 3D entangled network and also to its interaction with the inorganic phase [78]. Indeed carboxyl groups of the CMC may form strong ionic interaction especially with calcium ions of the apatite formed during the setting. In the present study, the introduction of

CMC as microspheres instead of raw powder enhanced the decrease of composite compressive strength probably due to the lower ability of CMC microspheres to form a polymer continuous network (CMC loose gel) within the mineral matrix. The lower availability of carboxyl groups of μ CMC-Ag to interact with calcium cations of the mineral matrix should also contribute in the decrease in the composite compressive strength as they were already involved in the interaction with silver cations within the microspheres [79-80]. Surprisingly, in the range of μ CMC-Ag content tested (2 and 10% of μ CMC-Ag in the composite) the correlation of C- μ CMC-Ag composites compressive strength to their respective porosity showed that the lower the porosity the lower the compressive strength contrary to what is generally observed for porous materials. It appears interesting to compare the mechanical properties of the C- μ CMC-Ag composites with other types of bone substitute materials. For example, Figure 9 shows a map of the elastic modulus and compressive strength of different biomaterials developed for bone tissue engineering and substitution. Interestingly, we can see that the C-REF' and the C- μ CMC-Ag composites position in terms of mechanical characteristics was close to that of cancellous bone and to dense biodegradable polymers. Considering the place of the porous biodegradable composites with lower mechanical properties (Figure 9), C-REF' and C-pCMC, C- μ CMC-Ag composites showed a good compromise between porosity and mechanical properties reaching cancellous bone mechanical properties.

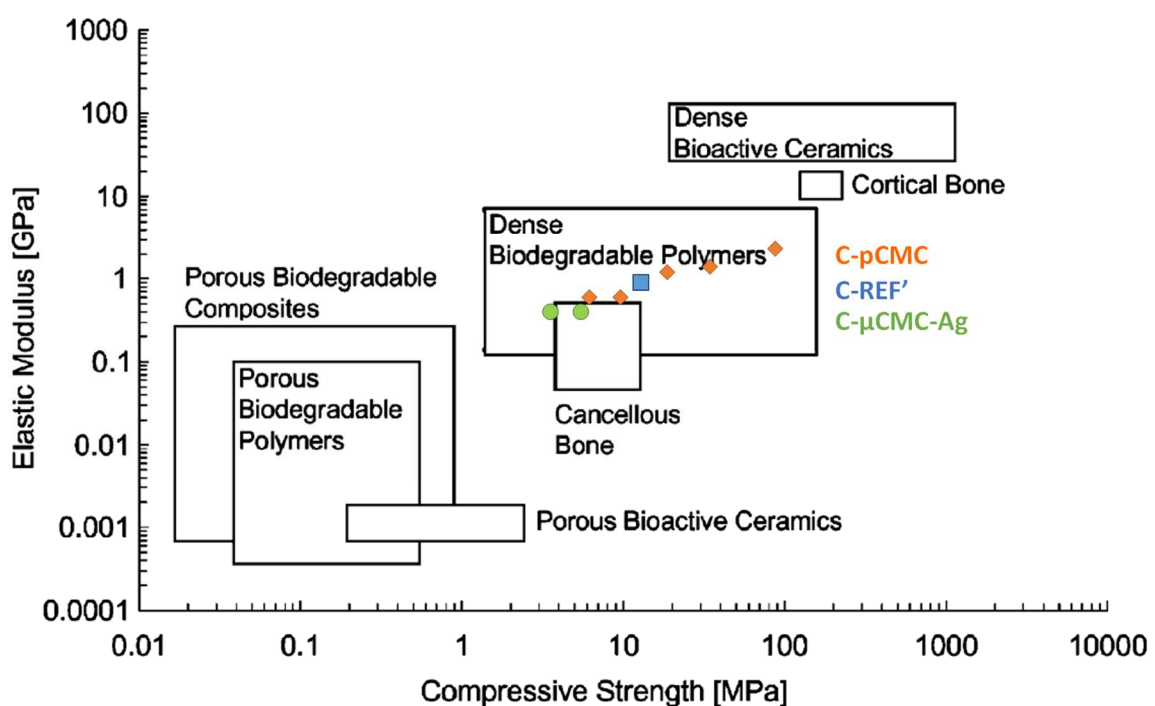


Figure 9: Young modulus of cements: C-REF' (square in blue), C-pCMC composites (diamonds in orange, composites for which CMC was introduced as raw powder from 2 to 50% (w/w) [78]) and C- μ CMC-Ag composites (disks in green, composites for which CMC was introduced as microspheres 2% and 10% (w/w)) as a function of their compressive resistance, compared with that of other biomaterials (from literature data on bioactive ceramics, biodegradable polymers and cancellous or cortical bone; adapted from Rezwan *et al.* [81]).

4. Conclusion

In this work, we carried out comparative studies to determine two silver salts' ability to confer an antibacterial activity to a mineral bone cement without affecting its biocompatibility, and how those silver salts could be loaded in the cement. Silver salts anti-biofilm activity appeared correlated both to their solubility in water, and their ability to interact with the cement mineral (micro)structure and its evolution during setting and hardening. We demonstrated that encapsulating soluble silver salts within spray-dried polysaccharide microspheres prior loading into the mineral cement could be an interesting strategy to avoid silver/calcium phosphate interaction during the setting step and thus to control silver release and reach more rapidly silver concentrations aimed to prevent bone-implant associated infection risk. Among the various forms of silver in medical devices (as solid: metallic nanoparticles and insoluble salts, as liquid: soluble ions), the question of the bioavailability and cytotoxicity of silver at the site of implantation is important to consider. Controlling the active dose delivered and its rate of delivery could be also interesting to limit the dose and its potential side effects.

After demonstrating the antibacterial and anti-biofilm activity of silver solutions, we were able to design cements containing efficient concentrations in silver salt(s) regarding biofilm formation inhibition for *S. aureus* CIP 4.83 and *S. epidermidis* CIP 6821T. We showed that the release of silver occurred over two weeks without burst effect and at a dose range conferring anti-biofilm efficiency without cytotoxicity. This targeted silver dose range was reached earlier (from $t = 3$ hours) for the C- μ CMC-Ag composite cement than for the C-Ag mineral cement (from day 1). Modelization of the silver release data for microsphere-loaded cement supported a higher release rate of silver that could be attributed to lower silver/mineral part interactions and to the presence of hydrophilic reservoir zones, leading more rapidly to

silver doses able to control biofilm formation by *S. aureus* and *S. epidermidis* in the cement microenvironment.

The development of injectable paste which can be implanted using mini-invasive surgery technique contributes also to the decrease in bone-implant infection risk. Our results demonstrated that the introduction of 2 or 10% silver-CMC microspheres in the cement formulation greatly improved its injectability and suppressed the filter-pressing phenomenon during paste extrusion.

The developed C- μ CMC-Ag biomimetic cement formulation including 10% (w/w) of μ CMC-Ag and thus 0.375% (w/w) of Ag appears promising as an antibacterial and injectable bone filling material able to reduce the risks of infection at the implantation site. Its implantation in animal model is currently under investigation.

Acknowledgements

The authors thank the Agence Nationale de la Recherche (ANR – TecSan 2009 program) for supporting this research work (BIOSINJECT project, grant n° ANR-09-TECS-004) and Françoise Maubé-Bosc (CIRIMAT, Toulouse) and Reine Bareille (BioTis, Bordeaux) for their help in the titration of silver by AA spectrometry and in hBMSCs cultures, respectively.

Authors contribution statement

Sylvaine Jacquart carried out the mineral and composite cement formulations and the physico-chemical characterization of the paste and set cements, Mohamed Fatnassi the CMC solutions rheological study and their spray drying, Robin Siadous the cytotoxicity experiments on silver salts, Christel Pigasse and Julien Grimoud the microbiological tests. Christian Rey co-supervised Sylvaine Jacquart and contributed in the cement characterization data analysis. Sophie Girod-Fullana and Fabien Brouillet co-supervised Mohamed Fatnassi research study (postdoc researcher) and performed the conceptualization of the CMC microparticles formulations, the silver release study and the modelization of the related data. Christine Roques conceptualized and coordinated the microbiological study and secure funding. Christèle Combes was the scientific coordinator of this research work and of the paper, she supervised Sylvaine Jacquart (PhD student) and secured funding. All authors contributed in the writing of this paper draft, read and approved this version of the manuscript.

References

- [1] R.O. Darouiche, Treatment of infections associated with surgical implants, *N. Engl. J. Med.* 350 (2004) 1422–1429. <http://dx.doi.org/10.1056/NEJMra035415>.
- [2] N.C.T. Dadi, B. Radochová, J. Vargová, H. Bujdáková, Impact of healthcare-associated infections connected to medical devices—An update, *Microorganisms* 9 (2021) 2332. <https://doi.org/10.3390/microorganisms9112332>.
- [3] A.J. Tande, R. Patel, Prosthetic joint infection, *Clin. Microbiol. Rev.* 27 (2014) 302–345. <http://dx.doi.org/10.1128/CMR.00111-13>.
- [4] M.R. Garner, S.A. Sethuraman, M.A. Schade, H. Boateng, Antibiotic prophylaxis in open fractures: Evidence, evolving issues, and recommendations, *J. Am. Acad. Orthop. Surg.* 28 (2020) 309–315. doi: 10.5435/JAAOS-D-18-00193.
- [5] G.M. Rossolini, F. Arena, P. Pecile, S. Pollini, Update on the antibiotic resistance crisis, *Curr. Opin. Pharmacol.* 18 (2014) 56–60. doi: 10.1016/j.coph.2014.09.006.
- [6] E. Martens, A.L. Demain, The antibiotic resistance crisis, with a focus on the United States, *J. Antibiot.* 70 (2017) 520–526. doi: 10.1038/ja.2017.30.
- [7] C. Wagner, G.M. Hänsch, Pathophysiology of implant-associated infections: From biofilm to osteolysis and septic loosening, *Orthopade.* 44 (2015) 967–973. doi: 10.1007/s00132-015-3183-z.
- [8] C. Wagner, G.M. Hänsch, Mechanisms of bacterial colonization of implants and host, *Adv. Exp. Med. Biol.* 971 (2017) 15–27. doi: 10.1007/5584_2016_173.
- [9] C.R. Arciola, D. Campoccia, L. Montanaro, Implant infections: adhesion, biofilm formation and immune evasion, *Nat. Rev. Microbiol.* 16 (2018) 397–409. doi: 10.1038/s41579-018-0019-y.
- [10] D. Campoccia, L. Montanaro, C.R. Arciola, A review of the biomaterials technologies for infection-resistant surfaces, *Biomaterials* 34 (2013) 8533–8554. doi: 10.1016/j.biomaterials.2013.07.089.
- [11] J. Hasan, R.J. Crawford, E.P. Ivanova, Antibacterial surfaces: the quest for a new generation of biomaterials, *Trends Biotechnol.* 13 (2013) 295–304. doi: 10.1016/j.tibtech.2013.01.017.
- [12] A. Shahid, B. Aslam, S. Muzammil, N. Aslam, M. Shahid, A. Almatroudi, K.S. Allemailem, M. Saqalein, M.A. Nisar, M.H. Rasool, M. Khurshid, The prospects of antimicrobial coated medical implants. *J. Appl. Biomater. Funct. Mater.* (2021) 1–21. doi: 10.1177/22808000211040304.
- [13] S. Eckhardt, P.S. Brunetto, J. Gagnon, M. Priebe, B. Giese, K.M. Fromm, Nanobio silver: Its interactions with peptides and bacteria, and its uses in medicine, *Chem. Rev.* 113 (2013) 4708 – 4754. <http://dx.doi.org/10.1021/cr300288v>.

- [14] K.M. Fromm, Silver coordination compounds with antimicrobial properties, *Appl. Organomet. Chem.* 27 (2013) 683–687. <http://dx.doi.org/10.1002/aoc.3047>.
- [15] S.L. Percival, W. Slone, S. Linton, T. Okel, L. Corum, J.G. Thomas, The antimicrobial efficacy of a silver alginate dressing against a broad spectrum of clinically relevant wound isolates, *Int. Wound J.* 8 (2011) 237–243. <http://dx.doi.org/10.1111/j.1742-481X.2011.00774.x>.
- [16] M.G. Gordienko, V.V. Palchikova, S.V. Kalenov, A.A. Belov, V.N. Lyasnikova, D.Y. Poberezhniy, A.V. Chibisova, V.V. Sorokin, D.A. Skladnev, Antimicrobial activity of silver salt and silver nanoparticles in different forms against microorganisms of different taxonomic groups, *J. Hazard Mater.* 378 (2019) 120754. doi: 10.1016/j.jhazmat.2019.120754.
- [17] Q.L. Feng, J. Wu, G.Q. Chen, F.Z. Cui, T.N. Kim, J.O. Kim, A mechanistic study of the antibacterial effect of silver ions on *Escherichia coli* and *Staphylococcus aureus*, *J. Biomed. Mater. Res.* 52 (2000) 662–668. DOI: 10.1002/1097-4636(20001215)52:4<662::aid-jbm10>3.0.co;2-3
- [18] P. Parvekar, J. Palaskar, S. Metgud, R. Maria, S. Dutta, The minimum inhibitory concentration (MIC) and minimum bactericidal concentration (MBC) of silver nanoparticles against *Staphylococcus aureus*, *Biomater. Investig. Dent.* 7 (2020) 105-109. doi: 10.1080/26415275.2020.1796674
- [19] P. Dibrov, J. Dzioba, K.K. Gosink, C.C. Hase, Chemiosmotic mechanism of antimicrobial activity of Ag in *Vibrio cholerae*, *Antimicrob. Agents Chemother.* 46 (2002) 2668–2670. <http://dx.doi.org/10.1128/AAC.46.8.2668-2670.2002>.
- [20] J. Dominguez-Herrera, F. Docobo-Perez, R. Lopez-Rojas, C. Pichardo, R. Ruiz-Valderas, J.A. Lepe, J. Pachon, Efficacy of daptomycin versus vancomycin in an experimental model of foreign-body and systemic infection caused by biofilm producers and methicillin-resistant *Staphylococcus epidermidis*, *Antimicrob. Agents Chemother.* 56 (2012) 613–617. <http://dx.doi.org/10.1128/AAC.05606-11>.
- [21] O. Gordon, T. Vig Slenters, P.S. Brunetto, A.E. Villaruz, D.E. Sturdevant, M. Otto, R. Landmann, K.M. Fromm, Silver coordination polymers for prevention of implant infection: Thiol interaction, impact on respiratory chain enzymes, and hydroxyl radical induction, *Antimicrob. Agents Chemother.* 54 (2010) 4208–4218. <http://dx.doi.org/10.1128/AAC.01830-09>.
- [22] D. Zhang, W. Liu, X.D. Wu, X. He, X. Lin, H. Wang, J. Li, J. Jiang, W. Huang, Efficacy of novel nano-hydroxyapatite/polyurethane composite scaffolds with silver phosphate particles in chronic osteomyelitis, *J. Mater. Sci.: Mater. Med.* 30 (2019) 59. doi: 10.1007/s10856-019-6261-7.

- [23] C. Bacali, I. Baldea, M. Moldovan, R. Carpa, D.E. Olteanu, G.A. Filip, V. Nastase, L. Lascu, M. Badea, M. Constantiniuc, F. Badea, Flexural strength, biocompatibility, and antimicrobial activity of a polymethyl methacrylate denture resin enhanced with graphene and silver nanoparticles, *Clin. Oral Investig.* 24 (2020) 2713-2725. doi: 10.1007/s00784-019-03133-2.
- [24] A. Masse, A. Bruno, M. Bosetti, A. Biasibetti, M. Cannas, P. Gallinaro, Prevention of pin track infection in external fixation with silver coated pins: Clinical and microbiological results, *J. Biomed. Mater. Res.* 53 (2000) 600–604. [http://dx.doi.org/10.1002/1097-4636\(200009\)53:5 600::AID -JBM21 3.0.CO;2-D](http://dx.doi.org/10.1002/1097-4636(200009)53:5 600::AID -JBM21 3.0.CO;2-D).
- [25] J. Hardes, C. von Eiff, A. Streitbuerger, M. Balke, T. Budny, M.P. Henrichs, G. Hauschild, H. Ahrens, Reduction of periprosthetic infection with silver-coated megaprotheses in patients with bone sarcoma, *J. Surg. Oncol.* 101 (2010) 389–395. <http://dx.doi.org/10.1002/jso.21498>.
- [26] H. Wafa, R.J. Grimer, K. Reddy, L. Jeys, A. Abudu, S.R. Carter, R.M. Tillman, Retrospective evaluation of the incidence of early periprosthetic infection with silver-treated endoprostheses in high-risk patients: Case control study, *Bone Joint J.* 97-B (2015) 252–257. DOI: 10.1302/0301-620X.97B2.34554.
- [27] R. Kuehl, P.S. Brunetto, A.K. Woischnig, M. Varisco, Z. Rajacic, J. Vosbeck, L. Terracciano, K.M. Fromm, N. Khanna, Preventing implant-associated infections by silver coating, *Antimicrob. Agents Chemother.* 60 (2016) 2467–2475. doi:10.1128/AAC.02934-15.
- [28] M.P. Ginebra, C. Canal, M. Espanol, D. Pastorino, E.B. Montufar, Calcium phosphate cements as drug delivery materials, *Adv. Drug Deliv. Rev.* 64 (2012) 1090-1110. doi: 10.1016/j.addr.2012.01.008.
- [29] M. Fosca, J.V. Rau, V. Uskoković, Factors influencing the drug release from calcium phosphate cements, *Bioact. Mater.* 7 (2022) 341-363. <https://doi.org/10.1016/j.bioactmat.2021.05.032>.
- [30] S. Jacquart, R. Siadous, C. Henocq-Pigasse, R. Bareille, C. Roques, C. Rey, C. Combes, Composition and properties of silver-containing calcium carbonate-calcium phosphate bone cement, *J. Mater. Sci.: Mater. Med.* 24 (2013) 2665-2675. <https://doi.org/10.1007/s10856-013-5014-2>.
- [31] J.V. Rau, M. Fosca, V. Graziani, A.A. Egorov, Y.V. Zobkov, Y.A. Fedotov, M. Orteni, R. Caminiti, A.E. Baranchikov, V.S.Komlev, Silver-doped calcium phosphate bone cements with antibacterial properties, *J. Funct. Biomater.* 7 (2016) 10. doi: 10.3390/jfb7020010.

- [32] S. Range, D. Hagemeyer, O. Rotan, V. Sokolova, J. Verheyen, B. Siebers, M. Epple, A continuous method to prepare poorly crystalline silver-doped calcium phosphate ceramics with antibacterial properties, *RSC Adv.* 5 (2015) 43172-43177. <https://doi.org/10.1039/C5RA00401B>.
- [33] P. Sikder, P.P. Coomar, J.M. Mewborn, S.B. Bhaduri, Antibacterial calcium phosphate composite cements reinforced with silver-doped magnesium phosphate (newberyite) micro-platelets, *J. Mech. Behav. Biomed. Mater.* 110 (2020) 103934. doi: 10.1016/j.jmbbm.2020.103934.
- [34] M. Honda, Y. Kawanobe, K. Nagata, K. Ishii, M. Matsumoto, M. Aizawa, Bactericidal and bioresorbable calcium phosphate cements fabricated by silver-containing tricalcium phosphate microspheres, *Int. J. Mol. Sci.* 21 (2020) 3745-3759. <https://doi.org/10.3390/ijms21113745>
- [35] V. Alt, T. Bechert, P. Steinrucke, M. Wagener, P. Seidel, E. Dingeldein, E. Domann, R. Schnettler, An in vitro assessment of the antibacterial properties and cytotoxicity of nanoparticulate silver bone cement, *Biomaterials* 25 (2004) 4383–4391. doi: 10.1016/j.biomaterials.2003.10.078.
- [36] M. Fatnassi, S. Jacquart, F. Brouillet, C. Rey, C. Combes, S. Girod Fullana,, Optimization of spray-dried hyaluronic acid microspheres to formulate drug-loaded bone substitute materials, *Powder Technol.* 255 (2014) 44-51. DOI:10.1016/j.powtec.2013.08.027.
- [37] M. Nouri-Felekori, M. Khakbiz, N. Nezafati, J. Mohammadi, B.M. Eslaminejad, Comparative analysis and properties evaluation of gelatin microspheres crosslinked with glutaraldehyde and 3-glycidoxypropyltrimethoxysilane as drug delivery systems for the antibiotic vancomycin, *Int. J. Pharm.* 557 (2019) 208-220. doi: 10.1016/j.ijpharm.2018.12.054.
- [38] R. Wu, B. Ma, Q. Zhou, C. Tang, Salmon calcitonin-loaded PLGA microspheres/calcium phosphate cement composites for osteoblast proliferation, *J. Appl. Polym. Sci.* 134 (2017) 45486. DOI: 10.1002/app.45486.
- [39] S.C. Yu, Y. Yu, H.L. Dai, Construction of gelatin microsphere / magnesium phosphate bone cement composite drug sustained delivery system, *J. Inorg. Mater.* 32 (2017) 655-660. DOI: 10.15541/jim20160553.
- [40] P.Q. Ruhe, O.C. Boerman, F.G.M. Russel, P.H.M. Spauwen, A.G. Mikos, J.A. Jansen, Controlled release of rhBMP-2 loaded poly(DL-lactic-co-glycolic acid)/calcium phosphate cement composites in vivo, *J. Control. Release* 106 (2005) 162-171. doi: 10.1016/j.jconrel.2005.04.018.

- [41] J. Schnieders, U. Gbureck, R. Thull, T. Kissel, Controlled release of gentamicin from calcium phosphate-poly(lactic acid-co-glycolic acid) composite bone cement, *Biomaterials* 27 (2006) 4239-4249. doi: 10.1016/j.biomaterials.2006.03.032.
- [42] W.J.E.M Habraken, L.T. de Jonge, J.G.C. Wolke, L. Yubao, A.G. Mikos, J.A. Jansen, Introduction of gelatin microspheres into an injectable calcium phosphate cement, *J. Biomed. Mater. Res. Part A* 87A (2008) 643-655. doi: 10.1002/jbm.a.31703.
- [43] S. Girod Fullana, H. Ternet, M. Frèche, J.L. Lacout, F. Rodriguez, Controlled release properties and final macroporosity of a pectin microspheres-calcium phosphate composite bone cement, *Acta Biomater.* 6 (2010) 2294-2300. doi: 10.1016/j.actbio.2009.11.019.
- [44] H. Liao, X.F. Walboomers, W.J.E.M. Habraken, Z. Zhang, Y. Li, D.W. Grijpma, A.G. Mikos, J.G.C. Wolke, J.A. Jansen, Injectable calcium phosphate cement with PLGA, gelatin and PTMC microspheres in a rabbit femoral defect, *Acta Biomater.* 7 (2011) 1752-1759. 10.1016/j.actbio.2010.12.020.
- [45] M. Bohner, U. Gbureck, J.E. Barralet, Technological issues for the development of more efficient calcium phosphate bone cements: A critical assessment, *Biomaterials* 26 (2005) 6423-6429. doi: 10.1016/j.biomaterials.2005.03.049.
- [46] M.H. Alkhraisat, C. Rueda, F.T. Mario, J. Torres, L.B. Jerez, U. Gbureck, E.L. Cabarcos, The effect of hyaluronic acid on brushite cement cohesion, *Acta Biomater.* 5 (2009) 3150-3156. DOI: 10.1016/j.actbio.2009.04.001
- [47] B.T. Smith, A. Lu, E. Watson, M. Santoro, A.J. Melchiorri, E.C. Grosfeld, J.J.J.P. van den Beucken, J.A. Jansen, D.W. Scott, J.P. Fisher, A.G. Mikos, Incorporation of fast dissolving glucose porogens and poly(lactic-co-glycolic acid) microparticles within calcium phosphate cements for bone tissue regeneration, *Acta Biomater.* 78 (2018) 341-350. doi: 10.1016/j.actbio.2018.07.054.
- [48] K. Kiminami, K. Nagata, T. Konishi, M. Mizumoto, M. Honda, K. Nakano, M. Nagaya, H. Arimura, H. Nagashima, M. Aizawa, Bioresorbability of chelate-setting calcium-phosphate cement hybridized with gelatin particles using a porcine tibial defect model, *J. Ceram. Soc. Japan* 126 (2018) 71-78. DOI <http://doi.org/10.2109/jcersj2.17197>.
- [49] Z. Yuan, P. Wei, Y. Huang, W. Zhang, F. Chen, X. Zhang, J. Mao, D. Chen, Q. Cai, X. Yang, Injectable PLGA microspheres with tunable magnesium ion release for promoting bone regeneration, *Acta Biomater.* 85 (2019) 294-309. <https://doi.org/10.1016/j.actbio.2018.12.017>.
- [50] R. Patel, M. Patel, J. Kwak, A.K. Iyer, R. Karpoornathd, S. Desai, V. Rarh, Polymeric microspheres: A delivery system for osteogenic differentiation, *Polym. Adv. Technol.* 28 (2017) 1595-1609. DOI: 10.1002/pat.4084.

- [51] N. Nezafati, M. Farokhi, M. Heydari, S. Hesaraki, N.A. Nasab, In vitro bioactivity and cytocompatibility of an injectable calcium phosphate cement/silanated gelatin microsphere composite bone cement, *Compos. B Eng.* 175 (2019) 107146. <https://doi.org/10.1016/j.compositesb.2019.107146>
- [52] E.A. Bayer, J. Jordan, A. Roy, R. Gottardi, M.V. Fedorchak, P.N. Kumta, S.R. Little, Programmed platelet-derived growth factor-BB and bone morphogenetic protein-2 delivery from a hybrid calcium phosphate/alginate scaffold, *Tissue Eng.: Part A* 23&24 (2017) 1382-1393. DOI: 10.1089/ten.tea.2017.0027.
- [53] C.W. Chang, Y.R. Wu, K.C. Chang, C.L. Ko, D.J. Lin, W.C. Chen, In vitro characterization of porous calcium phosphate scaffolds capped with crosslinked hydrogels to avoid inherent brittleness, *Ceram. Int.* 44 (2018) 1575-1582. <https://doi.org/10.1016/j.ceramint.2017.10.077>.
- [54] S.M.H. Dabiri, A. Lagazzo, B. Aliakbarian, M. Mehrjoo, E. Finocchio, L. Pastorino, Fabrication of alginate modified brushite cement impregnated with antibiotic: Mechanical, thermal, and biological characterizations, *J. Biomed. Mater. Res.* 107A (2019) 2063–2075. DOI: 10.1002/jbm.a.36719.
- [55] K.H. Khayat, Viscosity-enhancing admixtures for cement-based materials - An overview, *Cem. Concr. Compos.* 20 (1998) 171-188. [https://doi.org/10.1016/S0958-9465\(98\)80006-1](https://doi.org/10.1016/S0958-9465(98)80006-1).
- [56] G. Yan, B. Chen, X. Zeng, Y. Sun, X. Tan, L. Lin, Recent advances on sustainable cellulosic materials for pharmaceutical carrier applications, *Carbohydr. Polym.* 244 (2020) 116492. <https://doi.org/10.1016/j.carbpol.2020.116492>.
- [57] F. Calegari, B.C. da Silva, J. Tedim, M.G.S. Ferreira, M.A.C. Berton, E.B. Marino, Benzotriazole encapsulation in spray-dried carboxymethylcellulose microspheres for active corrosion protection of carbon steel, *Prog. Org. Coat.* 138 (2020) 105329. DOI: 10.1016/j.porgcoat.2019.105329.
- [58] J. Vilamitjana-Amédée, R. Bareille, F. Rouais, A.I. Caplan, M.F. Harmand, Human bone marrow stromal cells express an osteoblastic phenotype in culture, *In Vitro Cell Dev. Biol. Anim.* 29A (1993) 699-707. doi: 10.1007/BF02631426.
- [59] C.R. Parish, A. Mullbacher, Automated colorimetric assay for T cell cytotoxicity, *J. Immunol. Methods* 58 (1983) 225-237. DOI: 10.1016/0022-1759(83)90277-6.
- [60] T. Mosmann, Rapid colorimetric assay for cellular growth and survival: Application to proliferation and cytotoxicity assays, *J. Immunol. Methods* 65 (1983) 55-63. doi: 10.1016/0022-1759(83)90303-4.

- [61] A. Brochot, A. Guilbot, L. Haddioui, C. Roques, Antibacterial, antifungal, and antiviral effects of three essential oil blends, *Microbiology Open* 6 (2017) e459. <https://doi.org/10.1002/mbo3.459>.
- [62] H. Ibrahim, A. Furiga, E. Najahi, C. Pigasse Hénocq, J.P. Nallet, C. Roques, A. Aubouy, M. Sauvain, P. Constant, M. Daffé, F. Nepveu, Antibacterial, antifungal and antileishmanial activities of indolone-N-oxide derivatives, *J. Antibiot.* 65 (2012) 499–504. DOI:10.1038/ja.2012.60.
- [63] C. Campanac, L. Pineau, A. Payard, G. Baziard-Mouysset, C. Roques, Interactions between biocide cationic agents and bacterial biofilm, *Antimicrob. Agents Chemother.* 46 (2002) 1469-1474. <https://doi.org/10.1128/AAC.46.5.1469-1474.2002>.
- [64] H. Noukrati, S. Cazalbou, I. Demnati, C. Rey, A. Barroug, C. Combes, Injectability, microstructure and release properties of sodium fusidate-loaded apatitic cement as a local drug-delivery system, *Mater. Sci. Eng. C Mater. Biol. Appl.* 59 (2016) 177-184. doi: 10.1016/j.msec.2015.09.070.
- [65] Europe Co, editor. *European Pharmacopoeia 10th ed.*, Strasbourg, France, 2019.
- [66] T. Higuchi, Mechanism of sustained-action medication. Theoretical analysis of rate of release of solid drugs dispersed in solid matrices, *J. Pharm. Sci.* 52 (1963) 1145-1149. <https://doi.org/10.1002/jps.2600521210>.
- [67] N.A. Peppas, B. Narasimhan, Mathematical models in drug delivery: How modeling has shaped the way we design new drug delivery systems, *J. Control. Release* 190 (2014) 75-81. DOI: 10.1016/j.jconrel.2014.06.041.
- [68] V. Papadopoulou, K. Kosmidis, M. Vlachou, P. Macheras, On the use of Weibull function for the discernment of drug release mechanisms, *Int. J. Pharm.* 309 (2006) 44-50. doi: 10.1016/j.ijpharm.2005.10.044.
- [69] C. Nastruzzi, E. Esposito, R. Gambari, E. Menegatti, Kinetics of bromocriptine release from microspheres: Comparative analysis between different in vitro models, *J. Microencapsul.* 11 (1994) 565-574. doi: 10.3109/02652049409034995.
- [70] Y. Zhang, M. Huo, J. Zhou, A. Zou, W. Li, C. Yao, S. Xie, DDSolver: An add-in program for modeling and comparison of drug dissolution profiles, *AAPS J.* 12 (2010) 263-271. doi: 10.1208/s12248-010-9185-1.
- [71] A.B.D. Nandiyanto, K. Okuyama, Progress in developing spray-drying methods for the production of controlled morphology particles, *Adv. Powder Technol.* 22 (2011) 1-19. <https://doi.org/10.1016/j.appt.2010.09.011>.

- [72] R. Vehring, H. Snyder, D. Lechuga-Ballesteros, Spray Drying, in: S. Ohtake, K-I. Izutsu, D. Lechuga-Ballesteros (Eds.), *Drying Technologies for Biotechnology and Pharmaceutical Applications*, Wiley, 2020, pp. 179–216. <https://doi.org/10.1002/9783527802104.ch7>.
- [73] W. Liu, W.D. Wu, C. Selomulya, X.D. Chen, Uniform chitosan microparticles prepared by a novel spray-drying technique, *Int. J. Chem. Eng.* (2011) ID 267218. <https://doi.org/10.1155/2011/267218>.
- [74] C. Corsaro, G. Neri, A.M. Mezzasalma, E. Fazio, Weibull modeling of controlled drug release from Ag-PMA nanosystems, *Polymers* 13 (2021) 2897. <https://doi.org/10.3390/polym13172897>.
- [75] H. Lombois-Burger, P. Colombet, J.L. Halary, H. Van Damme, Kneading and extrusion of dense polymer–cement pastes, *Cem. Concr. Res.* 36 (2006) 2086-2097. DOI: 10.1016/j.cemconres.2006.08.001.
- [76] E. Fernández, S. Sarda, M. Hamcerencu, M.D. Vlad, M. Gel, S. Valls, R. Torres, J. López, High-strength apatitic cement by modification with superplasticizers, *Biomaterials* 26 (2005) 2289-2296. doi: 10.1016/j.biomaterials.2004.07.043.
- [77] A. Hebeish, M. Hashem, M.M. Abd El-Hady, S. Sharaf, Development of CMC hydrogels loaded with silver nano-particles for medical applications, *Carbohydr. Polym.* 92 (2013) 407-413. doi: 10.1016/j.carbpol.2012.08.094.
- [78] S. Jacquart, D. Poquillon, G. Dechambre, S. Cazalbou, C. Rey, C. Combes, Mechanical properties of self-setting composites: Influence of the carboxymethylcellulose content and hydration state, *J. Mater. Sci.* 51 (2016) 4296–4305. DOI 10.1007/s10853-016-9739-4.
- [79] M. Kawashita, M. Nakao, M. Minoda, H.M. Kim, T. Beppu, T. Miyamoto, , T. Kokubo, T. Nakamura, Apatite-forming ability of carboxyl group-containing polymer gels in a simulated body fluid, *Biomaterials* 24 (2003) 2477–2484. doi: 10.1016/s0142-9612(03)00050-4.
- [80] T.T. Nge, J. Sugiyama, Surface functional group dependent apatite formation on bacterial cellulose microfibrils network in a simulated body fluid, *J. Biomed. Mater. Res. Part A* 81 (2007) 124–134. doi: 10.1002/jbm.a.31020.
- [81] K. Rezwan, Q.Z. Chen, J.J. Blaker, A.R. Boccaccini, Biodegradable and bioactive porous polymer/inorganic composite scaffolds for bone tissue engineering, *Biomaterials* 27 (2006) 3413-31. doi: 10.1016/j.biomaterials.2006.01.039.

